4-1989

The Effect of Carboxylation of Styrene-Butadiene Latex on Binder Migration

Peter James Rudy
Western Michigan University

The Effect of Carboxylation of Styrene-Butadiene Latex on Binder Migration

by

Peter James Rudy

A thesis submitted
in partial fulfillment of
the course requirements for
The Bachelor of Science Degree

Western Michigan University
Kalamazoo, Michigan
April, 1989

ABSTRACT

A literature review was conducted concerning material related to carboxylation of styrene-butadiene latexes, binder migration, and binder migration measurement. Theory showed the process by which styrene and butadiene monomers contribute to make up the polymer chain and the effect of S/B ratio, particle size, crosslinking and carboxylation by vinyl acid addition type, level and location on the chain. Binder migration parameters related to coated surface and base sheet migration were addressed, as was viscosity control to reduce migration. Measurement types including attenuated total reflectance (ATR) using the fourier transform infrared (FTIR) were reviewed.

Based on the literature an experimental procedure was implemented to study the effect that increased carboxylation of S/B latexes had on binder migration. A series of five latex samples, varying in level of carboxylation, was used to prepare a calibration curve and used in standard coating formulations under migration inducing trials. Viscosity corrected and uncorrected sets were run with each trial on Mylar, high-size and low-size sheets. The migration of the binder was measured at the coated surface using the ATR-FTIR. Data from the trial was compared back to the calibration curve to quantify the surface binder amounts.

Results showed that as the level of carboxylation went up the amount of binder migration was reduced. In addition, the use of carboxylated latex in coatings tended to show better migration reducing results than just viscosity control alone. The use of the ATR-FTIR was shown to be effective for surface latex study.

TABLE OF CONTENTS

OBJECTIVE

To determine whether increased levels of carboxylation of styrene-butadiene latex, with all other related parameters being kept as constant as possible, will reduce binder migration in paper coating.

KEYWORDS

Binder Migration	Latex	Carboxylation
Styrene-Butadiene	FTIR	Viscosity
Coating Drying	Attenuated Total Reflectance	
Vinyl Acid	Emulsion Polymerization	

INTRODUCTION

This thesis attempts to quantify the relationship between increasing the level of carboxylation in a styrene-butadiene latex and its resultant effect on binder migration. This is to be done using attenuated total reflectance (ATR) on a fourier transform infrared (FTIR) spectroscopy instrument. The ability to put a number on a binder migration phenomenon, representing the actual amount of migration that occurs, will result in a better correlation between carboxylation level and its migration reducing ability. This will provide a better overall understanding of carboxylated styrene-butadiene latexes in paper coating.

BACKGROUND AND THEORETICAL DISCUSSION

LATEX HISTORY AND DEVELOPMENT

The early 1940's marked the appearance of styrene-butadiene latexes as a result of efforts to prepare synthetic rubber (1). The first use of styrene-butadiene latex as a binder in paper and paperboard coating formulations came in the early 1950's (2). The use since then has continued to grow to the point that today the paper industry is the second largest consumer of styrene-butadiene latexes.

Carboxylation of the latex, or the addition of vinyl acids to the polymer chain in the late 1950's improved the performance characteristics of latex (3). Previously non-carboxylated latexes

required post stabilization (4). The added ingredients to post stabilize and the breakdown of the post stabilized latex during use had detrimental effects on coating runnability parameters such as pH adjustment, starch compatibility, and blade runnability. The older latex mechanism also reduced various end use performances such as wet rub and binding power. Carboxylating the styrene-butadiene improved the stability without post stabilization. This reduced the problems associated with post stabilization and stabilizing the polymer particle with respect to mechanical, chemical, and temperature exposures.

CURRENT LATEX DEVELOPMENT

Currently latexes can be classified in one of three groups (5); conventional, alkali swellable, and alkali reactive. In addition, work on pigment reactive latex is ongoing (6). As shown in Figure 1, conventional latexes are carboxylated styrene-butadiene latexes that exhibit low to medium Brookfield viscosity response as pH is increased (7). Alkali swellable latexes show an increase in viscosity up to pH values of approximately 7 and then the rate of increase decreases above the pH 7 mark. Alkali reactive latexes will also increase in viscosity with increased pH. However their viscosity will level off and decrease slightly with pH above 7. This diversity is dependent in part on the type and placement of the vinyl acid used in carboxylation (in addition to crosslinking, S/B ratio, etc.) and results in a wide range of applications to which carboxylated styrene-butadiene latexes can be applied.

Figure 1

Latex Groupings (6)

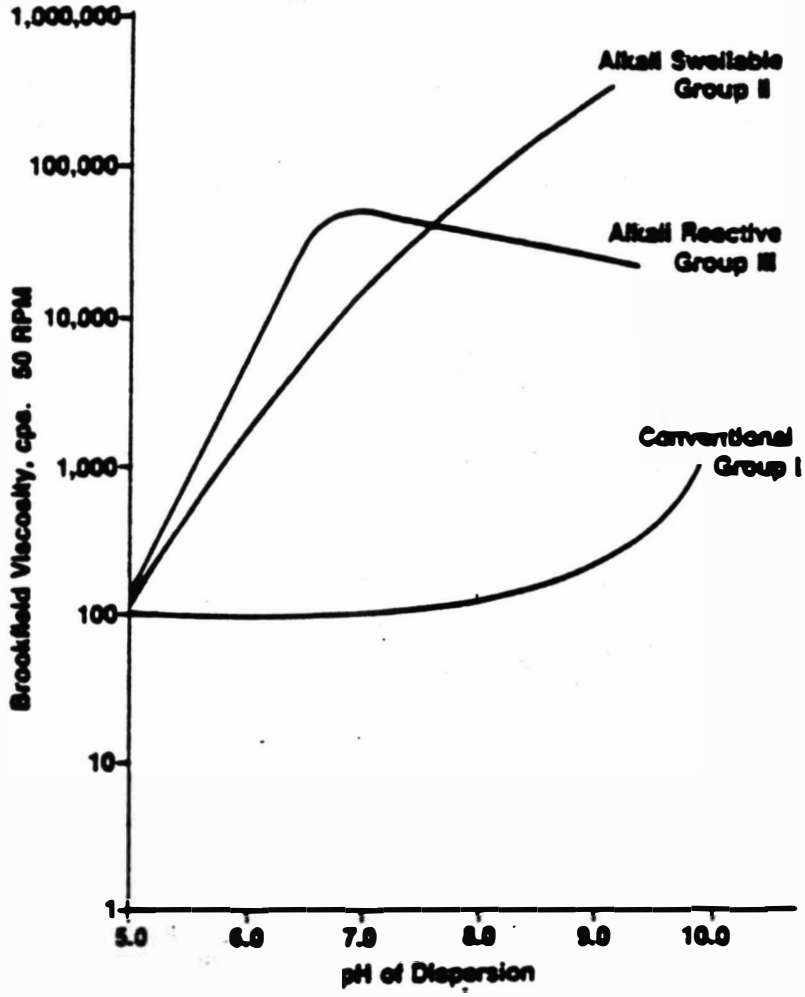

Figure 2

Styrene and Butadiene Monomers (8)

Figure 3

Styrene-Butadiene Polymer (8)

CARBOXYLATED STYRENE-BUTADIENE LATEX THEORY

To better understand carboxylated latex it is important to know the processes and theory used to make these polymers. A latex is a dispersion of finely divided, spherical polymer particles suspended in water, usually around a 50% polymer solids concentration (8). The particle size of the polymer generally ranges from 1000 angstroms to 3000 angstroms (9). The particle size, composition, molecular weight, and degree of crosslinking of the polymer sphere can all be controlled during polymer formation by the process of free radical emulsion polymerization. A quick review of this process reveals three mechanisms by which the polymer is formed from the available monomer units:

1) Initiation, which generates the free radicals necessary to start monomer polymerization.
2) Propagation, in which successive monomer addition promotes polymer chain growth.
3) Termination, which uses bimolecular transfer (via disproportionation or combination) or chain transfer to stop chain growth.

Emulsion polymerization is the best polymer formation process (4) because an emulsion is desired. Also it is more convenient to obtain small particle size and high molecular weights using this process. The monomer units of styrene-butadiene latexes are shown in Figure 2. Styrene monomer contributes the hard, inflexible,

however stable, nature to a polymer while the contributions of butadiene are tackiness, softness, elasticity, and flexibility. A typical styrene-butadiene copolymer is shown in Figure 3. The two monomers can be copolymerized with varying styrene-butadiene (S/B) ratios giving a wide range of properties.

A very important property of latex systems is colloidal stability (4). Stability is a function of:

1) Carboxylation - significantly enhances stability.
2) Particle size - larger particle size gives more stability.
3) Particle composition - harder latex spheres give better stability (to a limit).
4) The emulsifier type gives stability.

As shown in Figure 4, early latex particles achieved stability by using a post stabilization surfactant consisting of a hydrophobic end adsorbed on the particle surface and a hydrophilic tail pointing out towards the aqueous phase. Also, anionic surfactants were used, giving ionic repulsion stabilization. This is a relationship based on physical attraction and so severe agitation or desorbtion by addition of clays, starches, etc., could remove the surfactant and lessen particle stability.

Carboxylation of a styrene-butadiene copolymer involves polymerizing small amounts of mono or dicarboxylic vinyl acids into the polymer chain (3). Figure 5 shows some of these acid types. The amount is usually less than 10% (10), since too much impairs the polymer's elasticity, causes excessive latex swelling, and raises

Figure 4

Carboxylated and Noncarboxylated Latex (4)

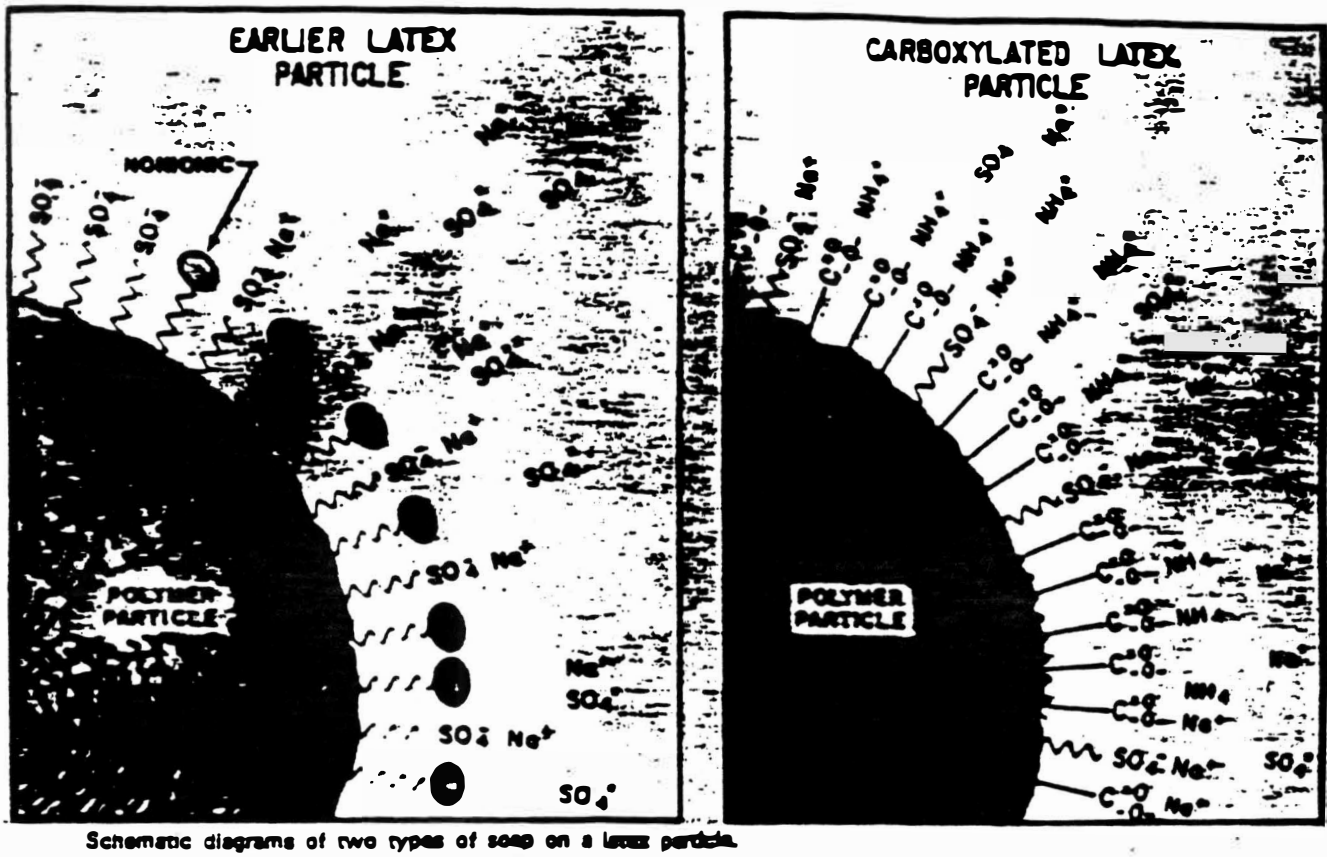

Schematic diagrams of two types of soap on a latex particle.

Figure 5

Vinyl Acid Types (3)

1. $CH_2 = CHC(=O)-OH$
Acrylic acid

2. $CH_2 = C(CH_3)-C(=O)-OH$
Methacrylic acid

3. $CH_3CH = CH-C(=O)-OH$
Crotonic acid

4. $CH_3CH = CHCH = CH-C(=O)-OH$
Sorbic acid

5. $CH_2 = C(-C(=O)-OH)-CH_2-C(=O)-OH$
Itaconic acid

6. $HO-C(=O)-CH = CH-C(=O)-OH$
Fumaric acid

the cost. The addition of the COOH groups provides chemically reactive sites in the polymer chains. The carboxylated latex particle shown in Figure 4 achieves stability by the ionization of the polymerized carboxyl groups on the outside of the particle surface towards the aqueous phase. The ionization of the carboxyl groups stabilizes the particle by forming a shell of water due to their hydrophilic nature. Stability is also obtained by the COOH groups development of electrostatic charges and resultant repulsion forces between particles. This makes them more stable against shear forces and other ingredient addition.

Vinyl acid additions to carboxylate the polymer chain are important with respect to type, level, and position (3). In simple carboxylated latexes, viscosity undergoes large increases when a high degree of COOH incorporation is used. Figure 6 shows this simple relationship. However, the type and level of vinyl acid can determine the type of latex response and so the final paper coating viscosity (2). The position of the vinyl acid can be one or a combination of five possible locations (3):

1) Within the particle, affecting particle hardness.
2) Copolymerized into the particle surface, increasing stability.
3) Adsorbed onto the particle surface, acting like a post stabilized latex.
4) As a soluble vinyl acid salt, with possible functions of pigment dispersant or thickener.
5) As an unreacted vinyl acid.

Figure 6

Carboxylation vs. Viscosity (9)

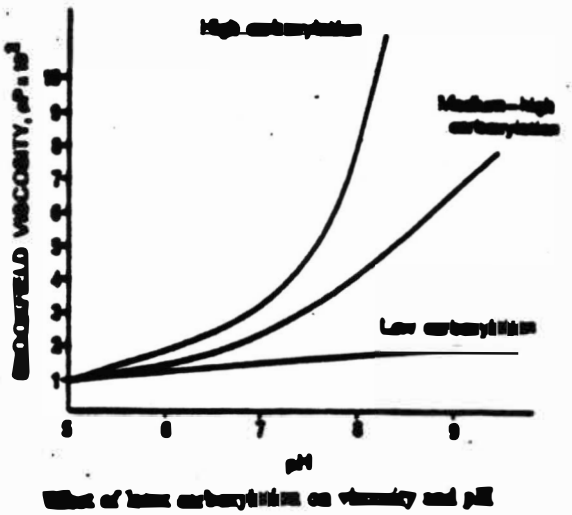

Figure 7

Carboxylation Positions (3)

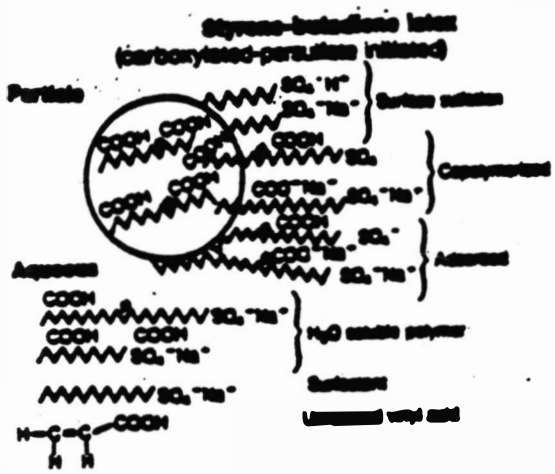

Figure 7 illustrates these five possibilities. Bound vinyl acids are more desirable since they contribute to the latex stability and enhance performance. The alkali swellable and alkali reactive latexes distinguish two types of viscosity responses that are obtained by manipulating the composition of the polymer, vinyl acid type, vinyl acid level, location, and particle size.

In addition to the previously mentioned parameters, carboxylated styrene-butadiene latex performance is affected by Tg of the polymer, molecular weight, film formation ability and gel formation ability. Tg, or the glass transition temperature, is the temperature at which the polymer undergoes a transition from a hard, glassy state to a soft rubbery state (9). In styrene-butadiene latexes the higher the percent styrene the higher the Tg (11). Tg relates to the composition and structure of the polymer. Film formation occurs during drying, when the compressive forces on the close-packed particles, caused by capillary and surface tension forces, are greater than the modulus of the latex polymer (12). Film formation is related to the Tg and the particle size, since smaller particles exhibit greater surface tension forces. Gel formation is defined as the formation of chemical bonds between polymer chains and particles that lead to possible infinite networks (9).

BINDER MIGRATION THEORY

Binder migration is the redistribution of the binder in the applied coating which can cause concentration gradients in the MD,

CD, or Z direction. Binder migration and its effects are observed with mottle, low gloss, and reduced pick strength. Binder migration has been classified as a mass transport phenomenon (13). It is more often studied as it relates to migration into the base sheet or to the coated surface. When directed towards the base sheet, the two forces that are responsible are capillary and pressure (14). Base sheet capillary action has been theorized to be surface tension controlled and pressure penetration to be viscosity controlled (15). When directed towards the surface, the mechanisms involved rely on one of two components (16). First, the effect of the evaporation rate on the liquid phase, and second the capillary transport of the liquid phase up to the coated surface during the consolidation process while drying. The two actions of migration towards the surface or towards the base sheet, when looked at with reference to the surface binder amounts, can result in too much or too little binder present at the surface for optimizing paper and printing characteristics. The migration of the binder can occur simultaneously in the MD, CD, and Z directions. This allows for the possibility of binder profile variations across the sheet.

PARAMETERS AFFECTING BINDER MIGRATION

Drying temperature has long been addressed in trying to control binder migration. This is because the evaporation rate traditionally was thought to drive binder migration. The ability to evenly heat and dry the coating throughout is most important if

binder migration is to be reduced. Cylinder dryers and hot air dryers have been shown to promote binder migration, even at air temperatures as low as 90 C (17). Infrared heaters have been reported to have less effect on binder migration due to their ability to heat the coating more evenly throughout because of no mass air flow (14).

Viscosity increases are traditionally used to reduce binder migration (18). High viscosities reduce binder migration by controlling the traditional force of liquid movement caused by water evaporation. Viscosity can be raised by either a percent solids increase, addition of a high molecular weight polymer, lowering the temperature, or use of a carboxylated latex. The most frequently used high molecular weight polymers are sodium alginate, carboxymethylcellulose (CMC), and hydroxyethylcellulose (HEC). HEC shows lower water retention values than the other two (19), probably due to the absence of carboxyl groups. However, HEC has been reported to give better overall results with respect to runnability, rheology, and final coat properties with an air knife study (20). The ability of carboxylated styrene-butadiene latex to increase viscosity is due to the higher water retention values and binder to pigment interactions of the swollen polymer particle (21). Particle size of the latex polymer plays a part in reducing binder migration too. Large particles tend to migrate less than small particles due to their physical size not allowing easy movement through the coating structure. The degree of migration to the surface of the coating has been reported to be inversely proportional to the particle size of the latex binder (13).

Other variables that influence binder migration are choice of base stock, sizing in the paper and coat weight. Groundwood containing paper has been shown to be less sensitive to the migration vs. drying parameters than wood free papers (14). High sizing in the base sheet can reduce the capillary penetration forces of base sheet migration (16). Coat weight is related to surface migration problems in that increased coat weight tends to promote binder migration (3,17). This is due to the inability to evenly heat the coating and the longer time it takes to dry the coating.

BINDER MIGRATION MEASUREMENT

Early measurement techniques for binder migration included IGT pick resistance, K & N ink absorbtion, and gloss (13). K & N in particular was used based on the premise that a high amount of binder at the surface of the paper reduces the ink absorptivity of the sheet.

Various instrumental methods have been reported (22,23,24) for evaluation of the coating layer including use of the scanning electron microscope (SEM), electron spectroscopy for chemical analysis (ESCA), ultraviolet absorption, and infrared spectroscopy using attenuated total reflectance (ATR). SEM (13) enlarges a surface or cross-sectional view of the coating, allowing for a visual interpretation of the coating structure. ESCA is probably the most reliable method for surface analysis, analyzing sample data to a 50-100 angstrom depth (25). It can readily detect

migration of binder to the surface of the coated sheet. Ultraviolet absorption using an x-y stage thin layer chromatography (TLC) scanner has been reported (23) to provide the ability to profile the surface amounts of the binder present. ATR has been used to measure the surface amount of the binder (27) as an average amount present.

ATTENUATED TOTAL REFECTANCE INFRARED SPECTROSCOPY THEORY

Infrared spectroscopy is already the most common tool used to measure the composition of latex (8). Infrared (IR) spectroscopy uses the differences that exist in the molecular absorption of infrared radiation, due to various vibrational and rotational states, to qualitatively and quantitatively analyze a sample (25). The absorbance is measured across a range of frequencies. from 4000 to 400 cm-1. Quantitative IR interpretations use the equation:

$$A = abc$$

where:

A = absorbance

a = absorptivity

b = path length

c = concentration

To use IR quantitatively requires finding a suitable band from a particular component and then showing that the absorbance is

related to the concentration of that component. The advantage of the fourier transform infrared (FTIR) instrument is its ability to measure simultaneously all the resolution elements, which reduces the time required to derive a spectrum. In addition, FTIR improves the signal to noise ratio, allowing signal averaging by decreasing observation time.

Attenuated total reflectance allows using IR to measure the paper surface of a sample nondestructively (26). Figure 8 shows the internal reflector plate, which in giving multiple reflections of the IR beam allows for the analysis of the coated surface. The surface has to be sufficiently smooth which may require pressing of the sample. Although the intense bands for styrene-butadiene latex occur in strong absorption regions of clay and calcium carbonate, Figure 9 shows that relatively strong bands exist at approximately 1450 cm-1 that do not exist in clay. The wavenumber suggests this is an absorption of an aromatic, most probably from the styrene portion of the polymer (25). Figure 10 shows the sample holder which uses a pressure plate with tightening screws to hold the sample in place. It is important here to apply firm even pressure so that each sample is held against the crystal uniformly. This will reduce any variation in absorbance measurements from sample to sample because of voids between the crystal and the coated latex surface.

Figure 8

Multiple Reflector (26)

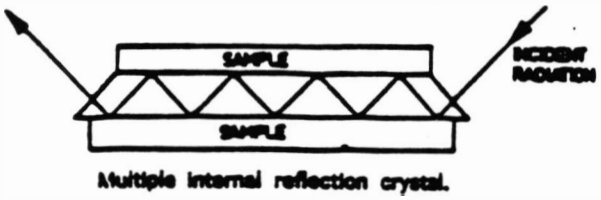

Multiple internal reflection crystal.

Figure 9

Styrene-Butadiene and Clay Absorbtion (26)

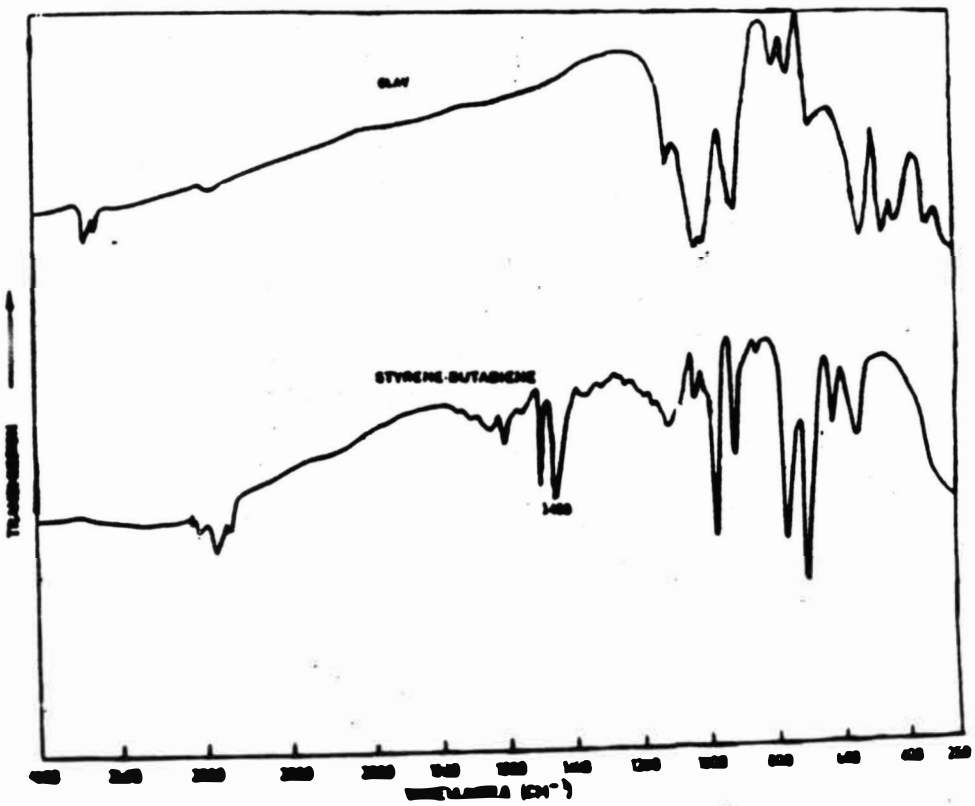

Figure 10

Sample Holder (26)

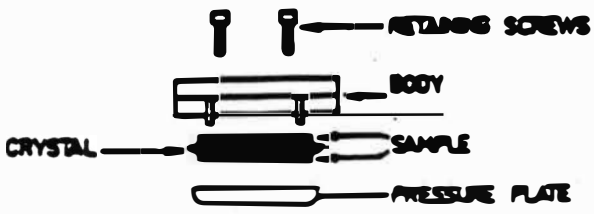

PRESENTATION OF PROBLEM

The objective of this thesis is to determine whether increased levels of carboxylation of styrene-butadiene latex will reduce binder migration in paper coating. Binder migration, or the movement of the binder throughout the coating including towards the surface and into the base sheet, is known to take place during the drying process. The harsher and more nonuniform the drying process, the more pronounced the binder migration. Viscosity control through the use of viscosity builders has traditionally been used to control binder migration. Carboxylated latexes have been increasingly used in coating formulations as a control measure for binder migration. Carboxylated latexes are known to increase viscosity and also are theorized to have added impact due to the effects of the COOH groups present in the latex. The experimentation here is to determine if in fact added carboxylation will decrease binder migration and if the carboxylation has some added impact as opposed to viscosity increase alone.

EXPERIMENTAL DESIGN

APPROACH

The experimental portion of this thesis will use a series of five latexes that vary in the level of carboxylation. The latexes are known to vary in carboxylation level up to approximately 15% (6). The vinyl acids groups used are the same for each latex except for the lowest carboxylated latex. All other parameters of the latex are as constant as can be expected. These latexes will be used to create calibration curves for each individual latex type. The latexes will then be run under binder migration inducing conditions using viscosity corrected and uncorrected sets. Measurement of the binder at the surface for the calibration curves and the binder migration runs will be done using infrared absorbance on the ATR-FTIR instrument. The calibration curves will be used to determine the amount of latex at the surface for the binder migration runs. Analysis of the effect of carboxylation level on binder migration and the effect of carboxylation vs. viscosity control will then be done.

VARIABLES TO CONTROL

To insure that the binder migration measured by the ATR-FTIR instrument, which measures at the surface of the coated sheet, is an accurate reflection of the effect of carboxylation alone, many variables that also contribute to binder migration will have to be

controlled. The effectiveness of the ATR-FTIR will depend on how well the mass transport phenomenon of binder migration is reflected by surface migration. It is desirable to achieve as much surface migration as possible. The parameters that promote migration into the sheet will have to be accounted for. This can be done by coating on Mylar, a high-size sheet, and a low-size sheet. Since Mylar has total resistance to coating penetration, comparisons can be made to correct for the flow of the binder into the high-size and low-size sheets.

Binder migration is known to be affected by coat weight, drying conditions, viscosity, and percent solids. These variables can be controlled to reduce error by proper technique during the coating application. In addition, the viscosity correction done to the viscosity controlled set will use HEC. This is because it has the performance characteristics needed plus the added benefit of not containing any carboxyl groups (as in CMC) which may possibly mimic the latexes water retention abilities.

MATERIALS AND CHEMICALS

1) Series of five carboxylated latexes (obtained from Dow Chemical Company).
2) Mylar (sheet and roll).
3) 800 HST and 400 HST sized 50/50 (BHW/BSW) paper. (HST = Hercules Size Test).
4) No. 2 clay.
5) Hydroxyethylcellulose (HEC).

6) Keegan coater, with forced hot air and infrared drying setup. (see Appendix 12).

7) Brookfield viscometer.

8) Drawdown blade and board.

9) NaOH for pH control.

10) Cowles mixer.

11) Small lightning mixer.

12) Nicolet ATR-FTIR instrument.

PROCEDURES

Calibration Curve Coating Application

A large batch of no. 2 clay was prepared at 70% solids using the Cowles mixer, mixing for 30 minutes. Using the series of five carboxylated latexes and the no. 2 clay, coatings were prepared at 55% total solids with 5%, 10%, 15%, 20%, 25%, and 30% latex (dry pigment weight basis). This was done for each of the five latexes. The coating was applied to Mylar sheets using a drawdown blade and allowed to air dry. A 15 lb/R (R=3000 sq. ft) coat weight was applied.

Binder Migration Run Coating Application

A large batch of no. 2 clay was prepared at 70% solids using the Cowles mixer, mixing for 30 minutes. Using the series of five carboxylated latexes and the no. 2 clay, two sets of coatings were

prepared at 65% total solids using each of the five latexes. To each coating 10% latex was added (dry pigment weight basis). The pH was adjusted to 8.0 for all coatings. Brookfield viscosity was taken for each latex type coating. All the coatings of one set were corrected to the highest viscosity present in the uncorrected set (the highest carboxylation level). The coatings were run on Mylar, high-size (800 HST), and low-size (400 HST) base sheets using the Keegan coater. The Keegan setup is shown in Appendix 12. The weights on the blade were changed to allow for various coat weights so as to match coat weights between formulations. The hot air dryer was run at the highest setting approximately 5 inches from the coating surface. The sheets were then one pass supercalendered at 40 psi and room temperature.

ATR-FTIR Measurement

A background scan was first taken. The ATR unit was mounted in place as described in appendix 9-1. Using the assignments menu, the resolution was set at 4 cm-1, the number of scans at 100, the autogain on, the y-axis to absorbance units, and the quantitative measurement to #3 (or peak height). Two 50mm X 30mm samples were cut and placed one on each side of the reflection plate. The plate screw was tightened with firm, even pressure. The scans were made and the absorbance at 1454.7 cm-1 was recorded.

PRESENTATION AND DISCUSSION OF RESULTS

The results of this study are heavily dependent on the ability of the ATR-FTIR to measure the latex at the surface of the coated sheet. Figure 11 shows a cross-section of a coated sheet and gives an indication of smoothness on a microscopic scale. Note the roughness of the uncoated side on the right side of the photograph vs. the relatively smoother coated and calendered left side of the photograph. The smoother the coating surface the more accurate the infrared measurement. This is due to a more intense infrared beam making its way through the ATR crystal.

Table 1 shows the difference in absorbance (at 2917.2 cm-1 and 1454.7 cm-1) between calendered and uncalendered sheets. Samples of both the calendered and uncalendered coated paper were used to measure repeated absorbances in an unmoved sample and in a sample that was remounted between absorbance measurements. This was done to check the ATR-FTIR instrument for its repeatability and precision. This data shows that surface smoothness is a high priority if consistent results are to be obtained. The standard deviation for the calendered sheets was much lower for the respective remounted and unmoved samples than for uncalendered sheets. The unmoved sample results for the uncalendered and calendered sheets show the precision of the ATR-FTIR instrument. The low standard deviation for the calendered sheet reflects precision within 2% given the best possible conditions. The remounted sample gives data points taken from areas close enough to be considered having like conditions and so presumed like binder

FIGURE 11
Cross-section Coated Paper

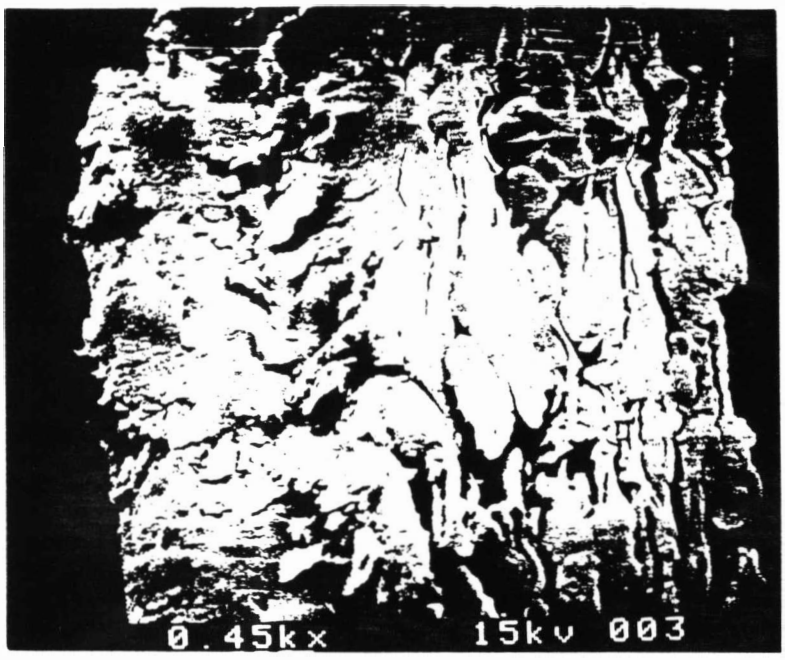

FIGURE 12
Low Size Sheet Surface Porosity

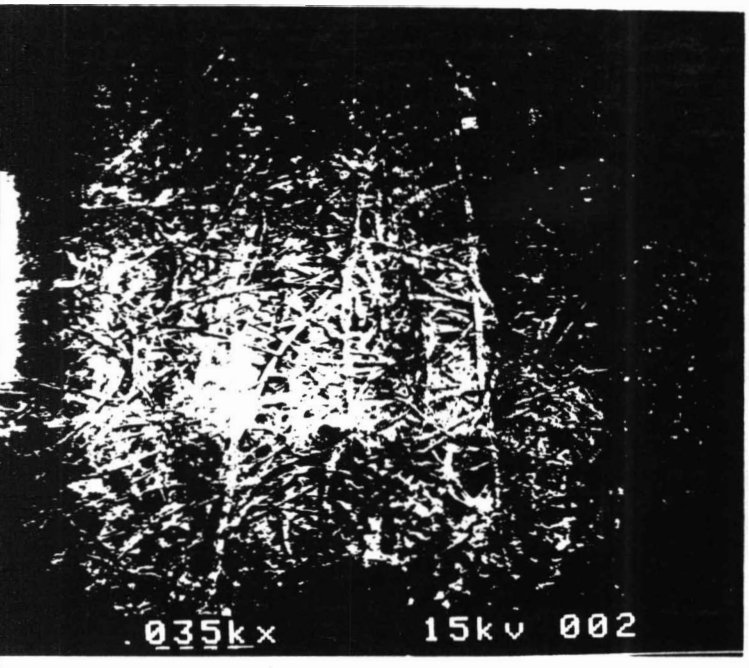

FIGURE 13
High Size Sheet Surface Porosity

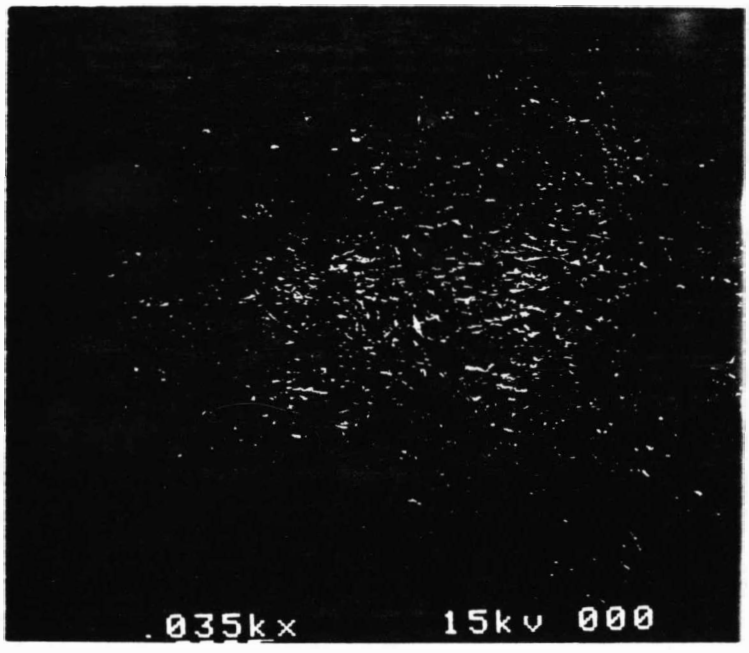

TABLE 1

REPEATABILITY TRIAL

UNCALENDERED SHEET
REMOUNTED SAMPLE

ABSORBANCE	2917.2	1454.7
T1	1.9445	1.0474
T2	2.0842	1.2110
T3	1.8299	1.0274
T4	1.7884	0.9661
T5	1.8142	0.9925
AVE.	1.8922	1.0489
STD. DEV.	0.1228	0.0959

UNCALENDERED SHEET
UNMOVED SAMPLE

ABSORBANCE	2917.2	1454.7
T1	1.8130	0.9886
T2	1.8180	1.0071
T3	1.8208	1.0114
T4	1.8213	1.0145
T5	1.8222	1.0177
AVE.	1.8191	1.0079
STD. DEV.	0.0037	0.0115

CALENDERED SHEET
REMOUNTED SAMPLE

ABSORBANCE	2917.2	1454.7
T1	1.0220	0.8597
T2	1.0646	0.9104
T3	1.0221	0.8712
T4	1.0227	0.8737
T5	1.0339	0.8842
AVE.	1.0331	0.8798
STD. DEV.	0.0183	0.0192

CALENDERED SHEET
UNMOVED SAMPLE

ABSORBANCE	2917.2	1454.7
T1	1.0182	0.8499
T2	1.0188	0.8465
T3	1.0189	0.8440
T4	1.0200	0.8435
T5	1.0199	0.8426
AVE.	1.0192	0.8453
STD. DEV.	0.0008	0.0030

migration amounts. This is a good indication of the repeatability of the ATR-FTIR instrument to measure a certain surface latex amount under changing mounting and surface conditions. The standard deviation here is larger which might indicate a decrease in precision if mounting and surface conditions change from sample to sample.

Table 2 gives the averages and the standard deviations for the calibration curve data. The standard deviations were higher for the data which indicates less precision than was shown possible in the repeatability trial. This is because the calibration curve coatings were not able to be calendered due to cracking of the dried coating on the Mylar sheets. The averages tended to fluctuate up and down between latex type within a certain percentage latex group. Table 3 gives averages based on all latex types for each percent latex amount. This was done to achieve a better calibration curve after analyzing statistically the independent calibration curves vs. an average calibration curve.

Table 4 gives the calculated least squares line data found using regression analysis (see Appendix 2). As shown, when regression fit based on the individual latex type was attempted using this data the R squared fit was not high (see graphs Appendix 8-1 to 8-5). The averages were based on only three data points and so if one absorbance measurement was out of line it tended to have a large impact on the average (see Appendix 1). This resulted in calibration curves that were not accurate enough to continue with comparison against the trial run data.

To achieve a better calibration curve, the data from all latex

TABLE 2

CALIBRATION CURVE DATA
AVERAGES
WAVELENGTH 1454.7

LATEX TYPE	A	B	C	D	E
PERCENT LATEX					
5.0000					
AVERAGE	0.8239	0.8216	0.8444	0.7714	0.8145
STD. DEV.	0.0413	0.0090	0.0194	0.0104	0.0175
COEFF. OF VAR.	5.0%	1.1%	2.3%	1.3%	2.1%
10.0000					
AVERAGE	0.8432	0.8443	0.8447	0.7805	0.7994
STD. DEV.	0.0433	0.0297	0.0200	0.0126	0.0067
15.0000					
AVERAGE	0.8516	0.8575	0.8435	0.8129	0.8718
STD. DEV.	0.0146	0.0190	0.0070	0.0522	0.0384
20.0000					
AVERAGE	0.8590	0.8807	0.8326	0.8102	0.8594
STD. DEV.	0.0410	0.0059	0.0272	0.0215	0.0521
25.0000					
AVERAGE	0.9536	0.9841	0.8783	0.8349	0.8607
STD. DEV.	0.0121	0.0420	0.0246	0.0248	0.0450
30.0000					
AVERAGE	1.0275	0.9617	0.8672	0.8824	0.8283
STD. DEV.	0.0165	0.0472	0.0431	0.0315	0.0521

TABLE 3

CALIBRATION CURVE DATA
ALL LATEX TYPES

PERCENT LATEX	AVERAGE	STD DEV	COEFF. OF VARIATION
5.0000	0.8152	0.0304	3.7%
10.0000	0.8224	0.0345	4.2%
15.0000	0.8475	0.0320	3.8%
20.0000	0.8484	0.0367	4.3%
25.0000	0.9027	0.0630	7.0%
30.0000	0.9134	0.0788	8.6%

TABLE 4

CALIBRATION CURVE LEAST SQUARES LINE
INDIVIDUAL LATEX CURVES

PERCENT LATEX	CALCULATED ABSORBANCES				
	A	B	C	D	E
5.0000	0.7962	0.8099	0.8374	0.7643	0.822(
10.0000	0.8352	0.8424	0.8434	0.7848	0.829(
15.0000	0.8742	0.8749	0.8494	0.8053	0.836(
20.0000	0.9132	0.9074	0.8554	0.8258	0.843(
25.0000	0.9522	0.9399	0.8614	0.8463	0.850(
30.0000	0.9912	0.9724	0.8674	0.8668	0.857(
R SQUARED	0.8256	0.8525	0.4011	0.9077	0.194

TABLE 5

CALIBRATION CURVE LEAST SQUARES LINE
COMBINED LATEX CURVES

PERCENT LATEX	CALCULATED ABSORBANCE
5.0000	0.8060
10.0000	0.8270
15.0000	0.8480
20.0000	0.8690
25.0000	0.8900
30.0000	0.9110

R SQUARED - 0.9167

types was used for an average as in Table 3. This is based on the assumption that the differences in absorption due to the composition of each latex carboxylation level would have less effect on error than the variability of averages based on only three data points. A statistical one way analysis of variance was done on each of the percentage levels to see if there was any difference between the groups of latex types (see Appendix 10-1 to 10-6). The results did show that in three of the six groups their was no difference between groups. Although this is not overwhelming, when taken in light of there being only three data points per latex type, the use of all the latex types within a percentage to create one calibration curve would seem more reasonable. Table 5 gives the least squares line data calculated using regression analysis using all the latex types as an average at each percentage (see Appendix 2). The R squared fit here is very good as indicated by the graph in Figure 14. The actual data points in Figure 14 are presented using squares while the R squared fit data has the best fit line going through it. The use of all the latex types to develop a calibration curve appears to be a better choice to accurately reflect the trial run comparisons.

Table 6 gives the averages and the standard deviations for the binder migration inducing trial runs. The coatings here were able to be calendered for better smoothness and, based on the lower standard deviations, the absorbance results reflected a higher degree of precision. The averages for each latex type and viscosity grouping were then compared against the calibration curve of Figure 14 to obtain percent latex at the surface of each coating type of

FIGURE 14

Regression curve fit using all latex averages

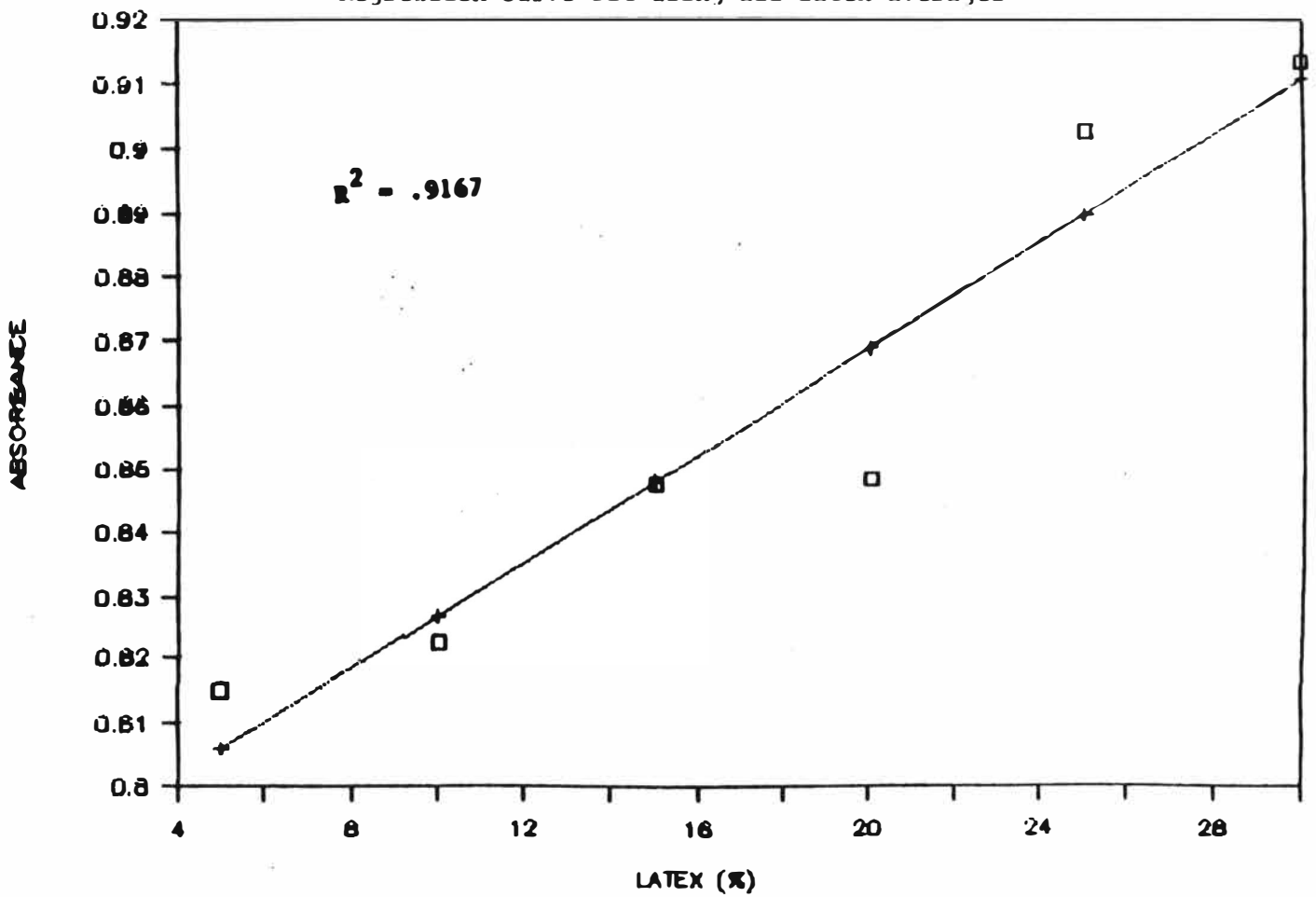

TABLE 6

EXPERIMENTAL RUN DATA
AVERAGES
WAVELENGTH 1454.7

LOW SIZE

LATEX TYPE	A	B	C	D	E
VISCOSITY UNCORRECTED					
AVERAGE	0.9591	0.8503	0.8828	0.8663	0.837
STD. DEV.	0.0849	0.0423	0.0353	0.0283	0.005
VISCOSITY CORRECTED					
AVERAGE	0.8764	0.9056	0.8843	0.8685	0.846
STD. DEV.	0.0088	0.0187	0.0098	0.0093	0.01

HIGH SIZE

LATEX TYPE	A	B	C	D	E
VISCOSITY UNCORRECTED					
AVERAGE	0.9362	0.9065	0.8844	0.8815	0.84
STD. DEV.	0.0424	0.0149	0.0132	0.0099	0.01
VISCOSITY CORRECTED - ALL 10% LATEX					
AVERAGE	0.8848	0.8807	0.8614	0.8643	0.86
STD. DEV.	0.0124	0.0041	0.0099	0.0079	0.01

MYLAR

VISCOSITY UNCORRECTED - ALL 10% LATEX					
AVERAGE	0.9510	0.9513	0.9492	0.9122	0.86
STD. DEV.	0.0156	0.0231	0.0159	0.0159	0.02
VISCOSITY CORRECTED - ALL 10% LATEX					
AVERAGE	0.9508	0.9455	0.9589	0.9552	0.96
STD. DEV.	0.0094	0.0209	0.0189	0.0472	0.00

the trials runs. This is presented in Table 7. Note that the data in Table 7 reflect a decrease in latex at the surface as the carboxylation goes up (the carboxylation values here represent increasing carboxylation as opposed to exact carboxylation level). Table 8 gives the calculated values for the best fit line of the viscosity corrected and uncorrected averages using regression analysis (see Appendix 4). The R squared values range from .5046 to .9454 with roughly three indicating fair to excellent fits and three indicating less than fair fits. The viscosity uncorrected averages generally had better fits than the viscosity corrected averages.

The graphs of Figures 15, 16, and 17 show the best line fits along with the data points for low-size, high-size, and Mylar sheets, respectively. In each case the line for the viscosity uncorrected coatings shows a decrease in binder at the surface as carboxylation goes up. Also in each case, the line for the viscosity corrected coatings is located below the viscosity uncorrected line with a smaller slope. A possible explanation for this is the viscosity correction has reduced the ability of the binder to migrate to the surface.

The graphs of Figures 15, 16, and 17 all reflect the same two trends. First, when the level of carboxylation goes up the amount of latex at the surface, or binder migration goes down. Second, it can be shown that based on the data carboxylation has a better migration reducing effect than just viscosity correction alone. The first trend was shown by the decrease in the amount of latex at the surface as the carboxylation level increased. This happened

TABLE 7

CALCULATED PERCENT LATEX FROM CALIBRATION CURVES
USING ALL TYPE LATEX DATA

CARBOXY. LEVEL	LOW SIZE UN	LOW SIZE CORR	HIGH SIZE UN	HIGH SIZE CORR	MYLAR UN	MYLAR CORR
1.0000	41.4444	21.7698	36.0000	23.7698	39.5317	39.4841
2.0000	15.5556	28.7143	28.9206	22.7857	39.6032	38.2222
3.0000	23.2937	23.6349	23.6587	18.1905	39.0952	41.3968
4.0000	19.3651	19.8810	22.9841	18.8889	30.2778	40.5159
5.0000	12.5079	14.5397	13.5397	20.0159	19.2540	42.6032

TABLE 8
CALCULATED LATEX RUN REGRESSION VALUES
USING ALL TYPE RUN AVERAGES

CARBOXY. LEVEL	LOW SIZE UN	LOW SIZE CORR	HIGH SIZE UN	HIGH SIZE CORR	MYLAR UN	MYLAR CORR
1.0000	33.2461	26.3666	35.1921	23.0111	43.5286	38.7381
2.0000	27.8398	24.0372	30.1064	21.8706	38.5405	39.5913
3.0000	22.4335	21.7078	25.0207	20.7301	33.5524	40.4445
4.0000	17.0272	19.3784	19.9350	19.5896	28.5643	41.2977
5.0000	11.6209	17.0490	14.8493	18.4491	23.5762	42.1509
R SQUARE	0.5649	0.5046	0.9454	0.3462	0.7817	0.6367

TABLE 9

BASE SHEET POROSITY TESTING
AVERAGE CALCULATIONS

BASE SHEET	GURLEY POROSITY	K and N REDUCTION	IMAGE AN. % POROSI
LOW SIZE	30.8	60.1	10.943
HIGH SIZE	24.3	62.0	15.594

FIGURE15

Regression fit for low size sheet using viscosity corr. and uncorr. coatings

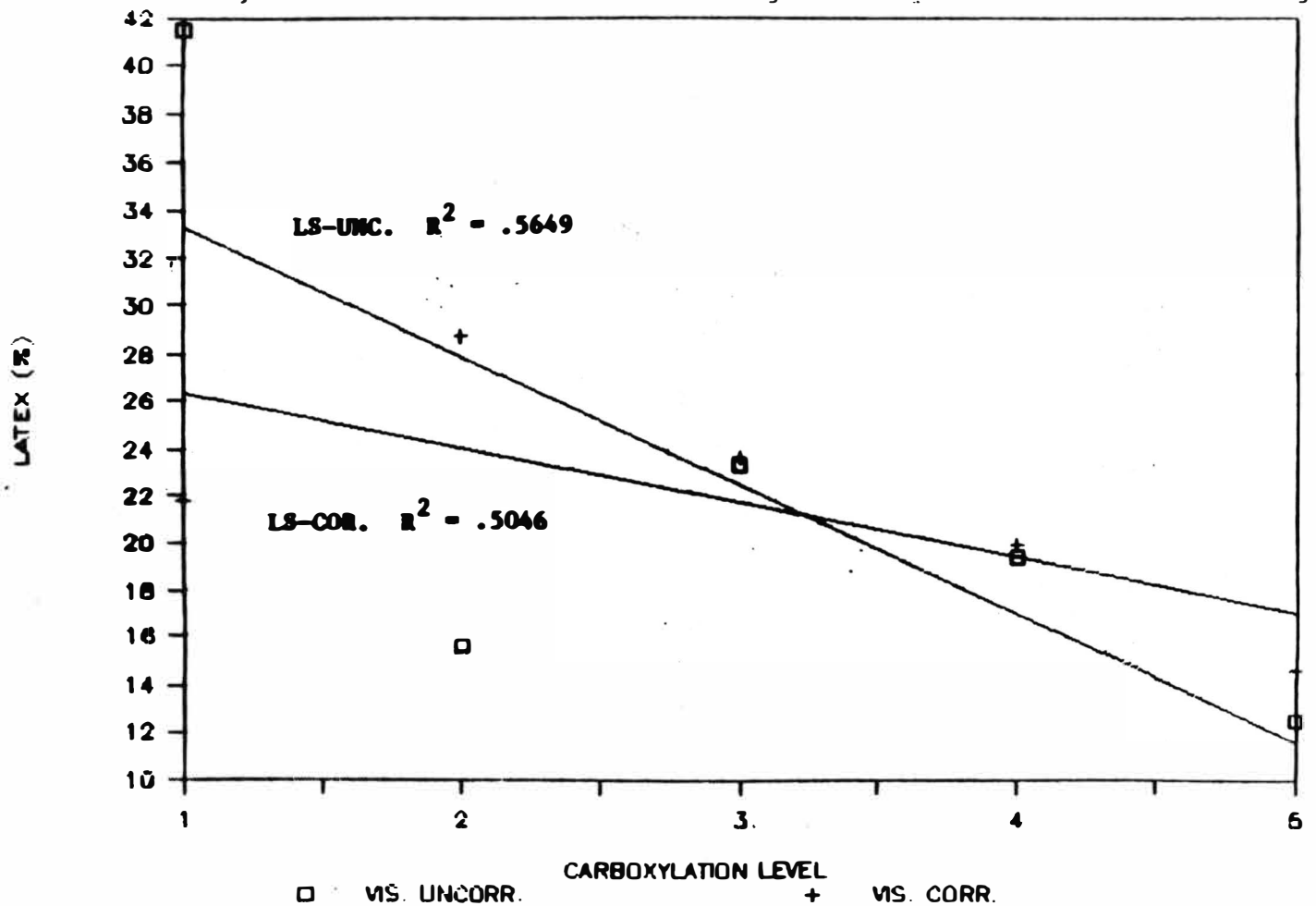

FIGURE 16

Regression fit for high size sheet using viscosity corr. and uncorr. coatings

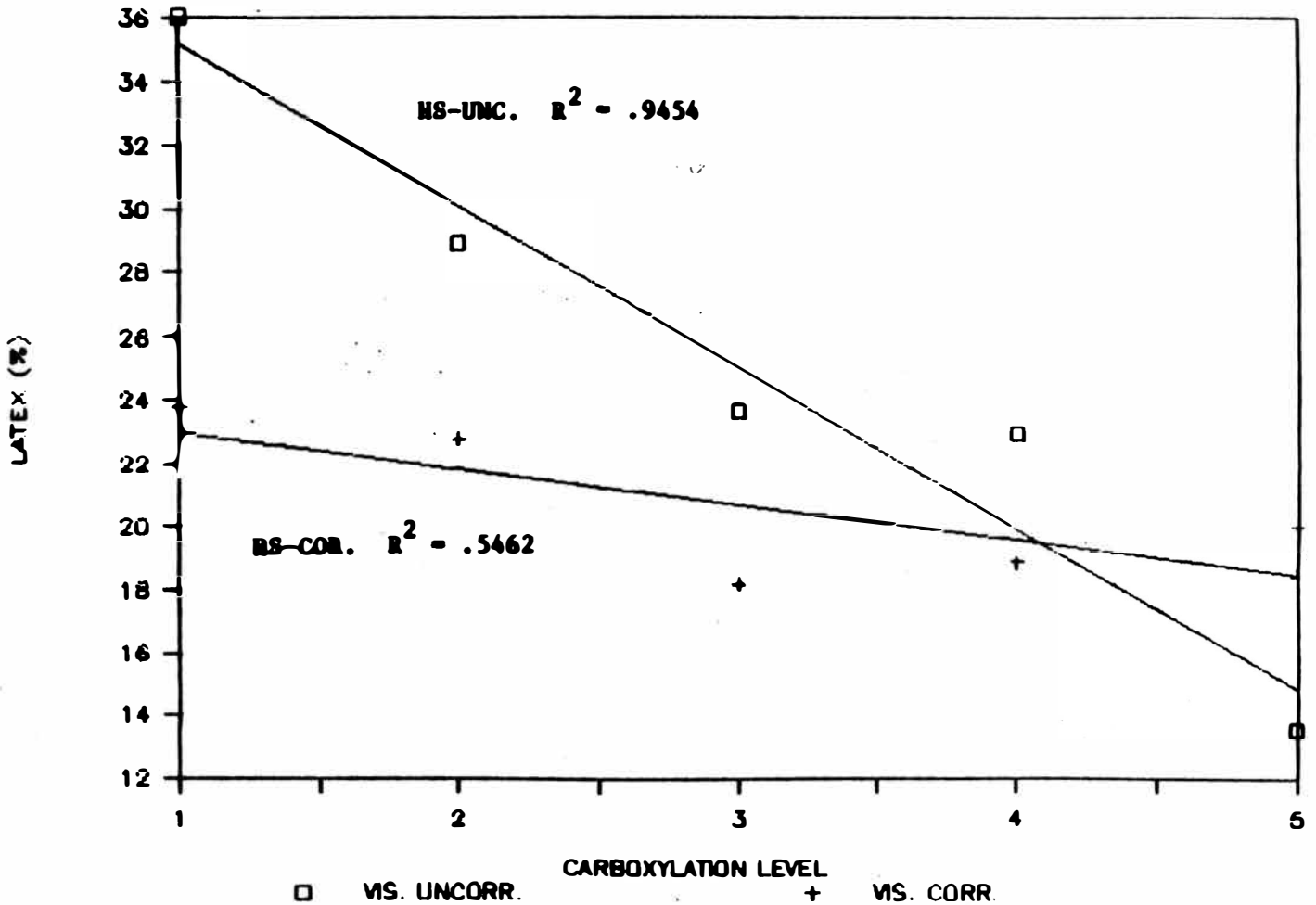

FIGURE17

Regression fit for mylar using viscosity corr. and uncorr. coatings

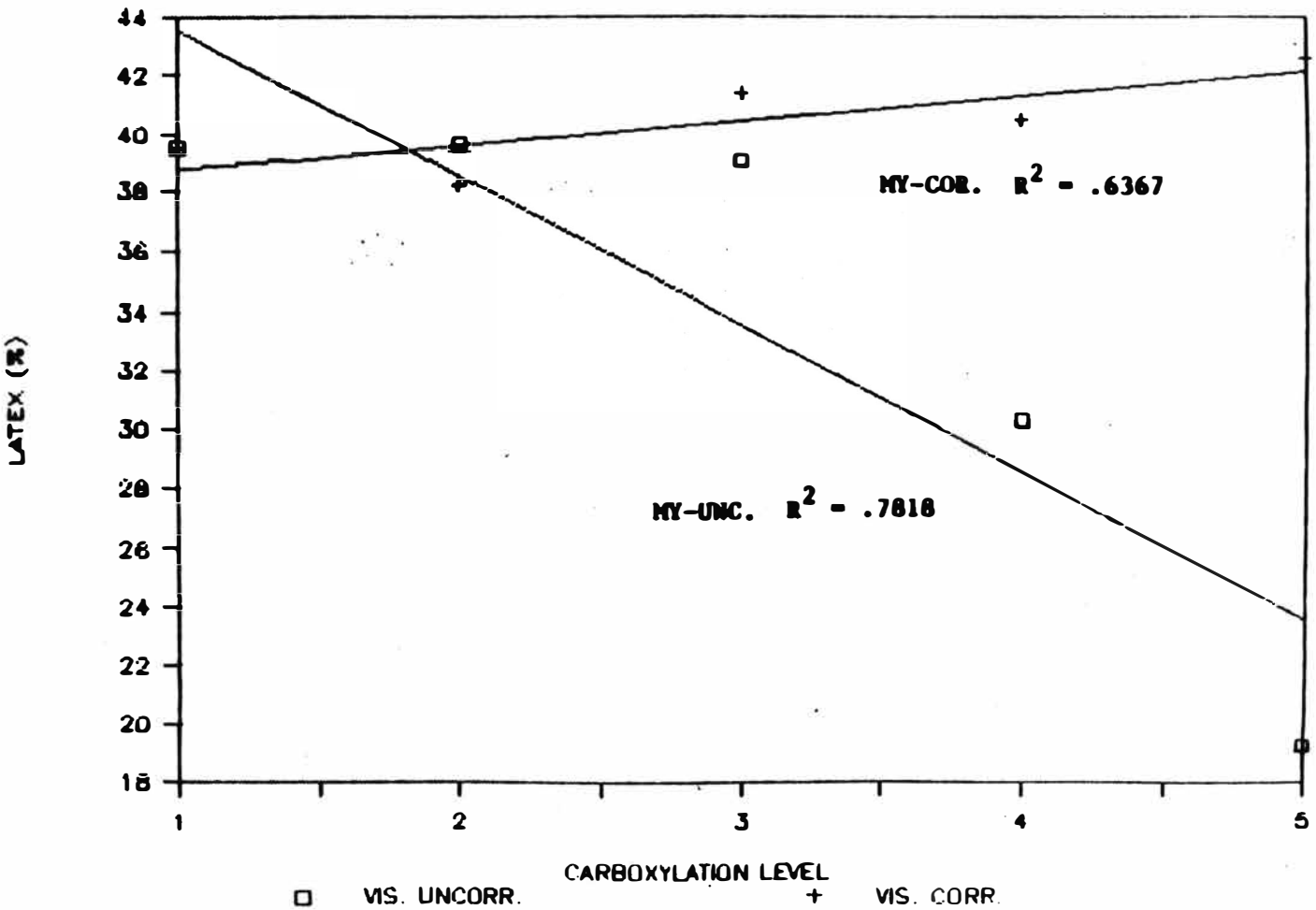

for each base sheet type. The increased carboxylation reduced the ability of the binder to migrate to the surface. Statistical analyses of the data using two way analysis of variance (see Appendix 11-1 to 11-3) show that there was a significant difference between latex types, which tends to support the hypothesis that of increased carboxylation reduced binder migration.

To show the second trend it is necessary to understand that the highest carboxylated latex (level 5) does not have any viscosity correction in the viscosity corrected group or in the viscosity uncorrected group. It is the same latex in each group. When the viscosity uncorrected group regression line shows a decrease in latex at the surface from the lowest carboxylation level to the highest carboxylation level, it represents the binder migration reducing ability due to increased carboxylation alone. The regression line of the viscosity corrected group also showed a decrease in latex amount at the surface as the level of carboxylation increased. However, if a base line is drawn from the highest carboxylation level data point across parallel to the X axis as in Figure 18, it can be seen that viscosity correction alone does not provide as much of a reduction in surface latex amount as does the carboxylation. This difference between this baseline and the viscosity corrected line is proposed to be the added impact of carboxylation on binder migration reduction over just viscosity correction alone. Statistical analyses of the data using two way analysis of variance (see Appendix 11-1 to 11-3) show that for two out of the three base sheet types a significant difference existed between viscosity corrected and viscosity

Figure 18
Effect of Carboxylation Using a Baseline
For a High-size Sheet

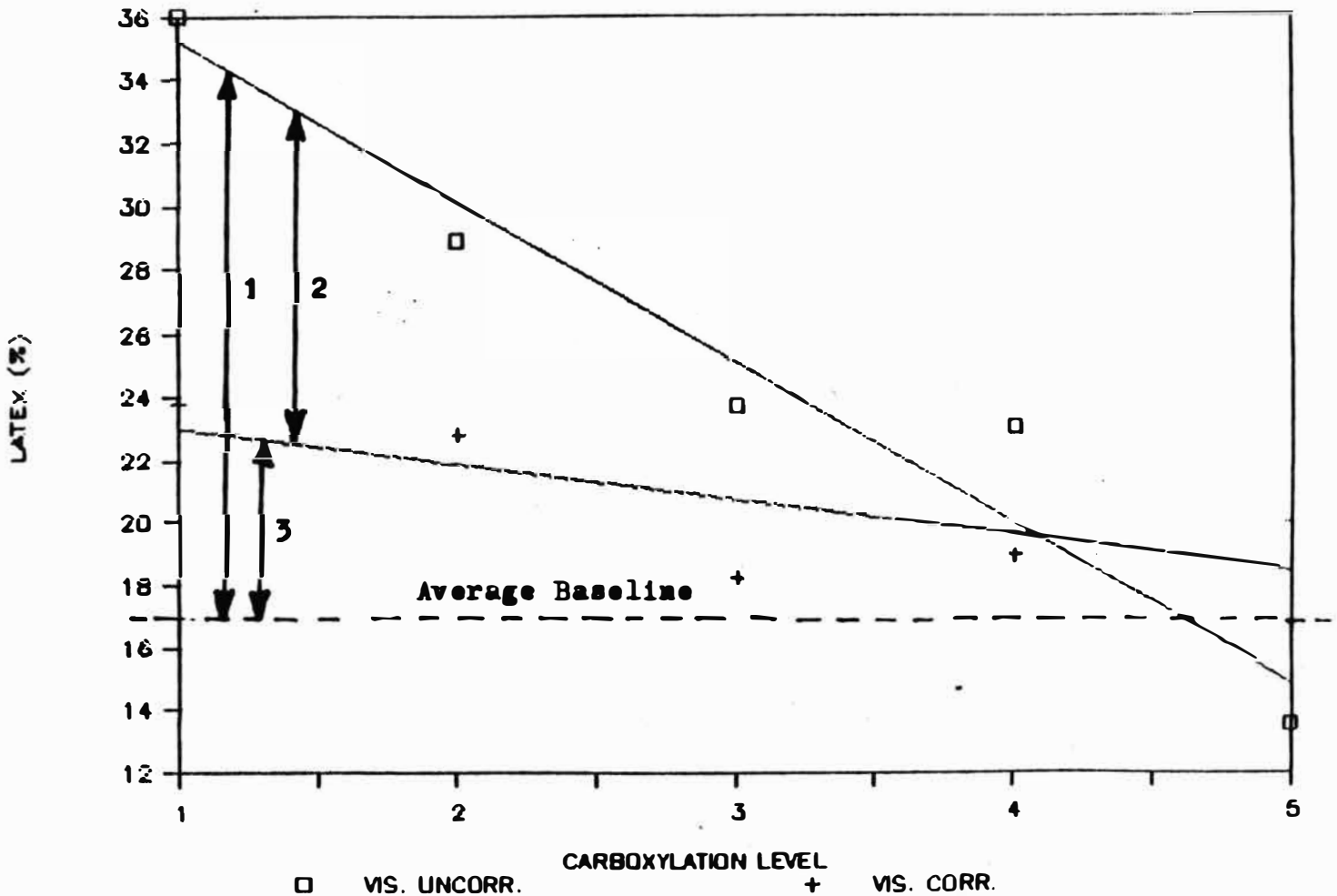

1) Effect of increased carboxylation on reducing binder migration.
2) Effect of viscosity correction on reducing binder migration.
3) Added effect of carboxylation over viscosity corrected latex on reducing binder migration.

uncorrected results. This tends to support the idea that carboxylation had an added effect over viscosity correction alone.

The coating applied to the Mylar gave higher amounts of latex at the surface overall than did the high size or low size sheets. Since Mylar has no penetration of coating or binder, this might be a reflection of how the blade pressure/porosity and capillary action/size parameters affect migration into the sheet. The Mylar certainly allows no penetration of the binder from either of the two parameters mentioned above. Comparing the Mylar results to the results of the high-size and low-size sheets gives interesting trends that possibly can shed some light on the interaction of the two parameters. The following discussion is hypothetical, however it might help to might explain the interaction.

The high size sheet was approximately 800 HST while the low size sheet was approximately 400 HST. Table 9 gives data for the low-size and high-size sheets based on Gurley porosity, K & N Ink brightness reduction, and percent surface porosity using the image analyzer. Porosity of the high-size sheet was found to be more than the porosity of the low-size sheet in each case. This can be seen clearly in the SEM photographs of Figures 12 and 13. It results from the lower internally sized low-size sheet picking up more surface starch at the size press than the high internally sized sheet. The high-size sheet is thus more likely to prevent penetration by capillary action and allow pressure penetration. The low-size sheet is more likely to do just the reverse when compared to the high-size sheet.

With this in mind it is interesting to note three trends

present. First, as the base sheets of low-size and high-size here are compared the porosity increases, respectively. Second, as the base sheets of high-size and low-size are compared the size decreases, respectively. Third, as the base sheets of high-size and low-size are compared the uncorrected latex amount at the surface decreases, respectively, which might indicate more binder migration into the low-size sheet. The viscosity uncorrected latex is used as an example because base sheet migration should be more evident in a viscosity uncorrected coating.

Since the lower porosity and low-sized sheet appeared to have more binder going into the sheet it might be reasoned that porosity had less of an effect than size with regard to binder migration. If porosity had a larger effect on the binder penetration or migration into the sheet, then the high-size sheet would show more penetration of the latex into the sheet and less on the surface. This is because the high-size sheet had larger pores to allow the pressure penetration to happen more readily and a higher size that would allow less capillary action penetration than the low-size sheet.

CONCLUSIONS

The results of this experimental work showed the tendency for surface binder migration to be reduced as the level of carboxylation in the coating latex increased and the tendency for carboxylation to reduce surface binder migration better than just viscosity correction alone. Also, the use of infrared spectroscopy using the ATR-FTIR instrument was shown to be promising for determining the amount of surface latex and so the amount of binder migration. Additional study is needed to improve the precision of the measurement.

RECOMMENDATIONS

Based on this work the use of carboxylated latexes over viscosity builders is recommended for paper coating use when the benefits outweigh the cost. The use of the ATR-FTIR is recommended and can be of value in defining the binder migration parameters. It has been shown to be effective in the measurement of the surface latex amount. Experimental techniques need to be refined relating to surface smoothness, sample mounting, etc.. Also, further study is dependent on producing a series of coatings that vary in latex amount and are homogenous throughout so that a dependable calibration curve can be established. Further study in this area is encouraged.

LITERATURE CITED

1) Jahn, R. G. and Hall, H. R., Synthetic and Protein Adhesives for Paper Coating, TAPPI Monograph 22, Chapter IV, TAPPI Press, N.Y., N.Y., (1961).

2) Hoover, J. F., TAPPI Seminar Notes, Coating Binders, pg 59 (1986).

3) Heiser, E. J., Pulp and Paper, pg 66 (May 1981).

4) Haig, S. H., and Heiser, E. J., Pulp and Paper Canada, 70 20: 10 (1969).

5) Purfeerst, R. D., and Willeamson G. D., Southern Pulp and Paper, pg 38 (June 1982).

6) Lichtenwald, K., Interview, Dow Chemical Company, (March 1989).

7) Purfeerst, R. D., and Williamson, G. D., Southern Pulp and Paper, pg 28 (May 1982).

8) von Gilder, R., Lee, D. I., Purfeerst, R. and Allsweede, J., Tappi Journal, 66 (11), 49 (1983).

9) Klun, R. R., TAPPI Seminar Notes, Coating Binders, pg 47 (1986).

10) Austin, J. G., Paper Technology, pg 200 (August 1974).

11) Ripley-Duggan, B. A., and Stickland, C. J., Paper Technology, pg 195 (August 1970).

12) Lee, D. I., Pulp and Paper, pg 55 (May 1975).

13) Heiser, E. J. and Baker, H. M., Tappi, 51 (11): (1968).

14) Eklund, D. E., and Palsanen, J. A., Tappi, 53 (10): 1925 (1970).

15) Clark, N. O., Windle, W. and Beazley, K. M., Tappi, 52 (11) 2191 (1969).

16) Engstrom, G., Strom, G., and Norrdahl, P., Tappi Journal, pg 45 (December 1987).

17) Thomin, W. H., Bergh, N. O., and Kogler, W. L., Tappi, 56 (1): 66 (1973).

18) Sinclair, A. R., Synthetic Binders in Paper Coatings, TAPPI Monograph 37, Chapter III, TAPPI Press, Atlanta (1975).

19) Bartell, D. G., Pulp and Paper Canada, 77 (7): 65 (1976).

20) Barber, E. J., and Bartell, D. G., Tappi, 59 (6): 123 (1976).

21) Essen, W. J., Erickson, D. E., and Rolik, M. A., Tappi, 50 (12): 622 (1967).

22) Heiser, E. J., Baker, H. M., and Herr, J. W., Tappi, 53 (9): 1739 (1970).

23) Kline, J. E., and Fujiwara, H., Research Paper, Western Michigan University, Dept. of Paper Science and Engineering.

24) Kline, J. E., and Fujiwara, H., International Process and Materials Quality Evaluation Conference, TAPPI Proceedings, pg157 (1986).

25) Hemminger, C. S., Coating Conference, TAPPI Proceedings, pg 55 (1985).

26) Skoog, D. A., "Principles of Instrumental Analysis", 3rd edition, Phil., CBS College Publishing (1985).

27) Michell, A. J., APPITA, 26 pg 25 (July 1972).

APPENDIX I

CALIBRATION CURVE DATA

WAVELENGTH 1454.7

LATEX TYPE	A	B	C	D	E
PERCENT LATEX	ABSORBANCE				
5.0000	0.8714	0.8204	0.8616	0.7834	0.7944
5.0000	0.8033	0.8133	0.8482	0.7647	0.8233
5.0000	0.7970	0.8312	0.8234	0.7660	0.8258
10.0000	0.8916	0.8220	0.8229	0.7744	0.7966
10.0000	0.8300	0.8330	0.8489	0.7721	0.7946
10.0000	0.8080	0.8780	0.8622	0.7950	0.8070
15.0000	0.8684	0.8357	0.8433	0.8697	0.8288
15.0000	0.8418	0.8666	0.8366	0.7671	0.9028
15.0000	0.8446	0.8702	0.8505	0.8020	0.8838
20.0000	0.8187	0.8820	0.8540	0.8343	0.8987
20.0000	0.8577	0.8858	0.8418	0.7928	0.8792
20.0000	0.9007	0.8743	0.8020	0.8035	0.8003
25.0000	0.9469	1.0264	0.8611	0.8074	0.8413
25.0000	0.9694	0.9424	0.8673	0.8416	0.9121
25.0000	0.9506	0.9836	0.9064	0.8557	0.8286
30.0000	1.0411	0.9072	0.9084	0.8472	0.7889
30.0000	1.0091	0.9880	0.8708	0.9080	0.8086
30.0000	1.0323	0.9898	0.8224	0.8921	0.8873

REGRESSION ANALYSIS CALCULATIONS

LATEX A

Regression Output:

Constant		0.7572	
Std Err of Y Est		0.0374	
R Squared		0.8256	
No. of Observations		6.0000	
Degrees of Freedom		4.0000	
X Coefficient(s)	0.0078		
Std Err of Coef.	0.0018		

LATEX B

Regression Output:

Constant		0.77	
Std Err of Y Est		0.02	
R Squared		0.85	
No. of Observations		6.00	
Degrees of Freedom		4.00	
X Coefficient(s)	0.0065		
Std Err of Coef.	0.0014		

LATEX C

Regression Output:

Constant		0.8314	
Std Err of Y Est		0.0149	
R Squared		0.4011	
No. of Observations		6.0000	
Degrees of Freedom		4.0000	
X Coefficient(s)	0.0012		
Std Err of Coef.	0.0007		

LATEX D

Regression Output:

Constant		0.74	
Std Err of Y Est		0.01	
R Squared		0.90	
No. of Observations		6.00	
Degrees of Freedom		4.00	
X Coefficient(s)	0.0041		
Std Err of Coef.	0.0007		

LATEX E

Regression Output:

Constant		0.8150	
Std Err of Y Est		0.0292	
R Squared		0.1942	
No. of Observations		6.0000	
Degrees of Freedom		4.0000	
X Coefficient(s)	0.0014		
Std Err of Coef.	0.0014		

ALL LATEX

Regression Output:

Constant		0.78	
Std Err of Y Est		0.0	
R Squared		0.9	
No. of Observations		6.0	
Degrees of Freedom		4.0	
X Coefficient(s)	0.0042		
Std Err of Coef.	0.0006		

EXPERIMENTAL RUN DATA

LOW SIZE
WAVELENGTH 1454.7

VISCOSITY UNCORRECTED - ALL 10% LATEX

LATEX TYPE	A	B	C	D	E
T1	0.9243	0.8920	0.9232	0.8952	0.83
T2	0.8971	0.8075	0.8579	0.8651	0.83
T3	1.0558	0.8515	0.8674	0.8387	0.84

VISCOSITY CORRECTED - ALL 10% LATEX

LATEX TYPE	A	B	C	D	E
T1	0.8784	0.9016	0.8849	0.8668	0.86
T2	0.8841	0.8892	0.8937	0.8602	0.83
T3	0.8668	0.9260	0.8742	0.8785	0.83

HIGH SIZE
WAVELENGTH 1454.7

VISCOSITY UNCORRECTED - ALL 10% LATEX

LATEX TYPE	A	B	C	D	E
T1	0.9837	0.9229	0.8695	0.8825	0.8
T2	0.9020	0.8940	0.8891	0.8712	0.85
T3	0.9229	0.9025	0.8945	0.8909	0.8

VISCOSITY CORRECTED - ALL 10% LATEX

LATEX TYPE	A	B	C	D	E
T1	0.8721	0.8768	0.8513	0.8707	0.85
T2	0.8855	0.8804	0.8618	0.8668	0.87
T3	0.8969	0.8849	0.8711	0.8555	0.88

MYLAR
WAVELENGTH 1454.7

VISCOSITY UNCORRECTED - ALL 10% LATEX

LATEX TYPE	A	B	C	D	E
T1	0.9618	0.9482	0.9618	0.9029	0.89
T2	0.9581	0.9300	0.9313	0.9031	0.8-
T3	0.9332	0.9758	0.9545	0.9305	0.86

VISCOSITY CORRECTED - ALL 10% LATEX

LATEX TYPE	A	B	C	D	E
T1	0.9574	0.9371	0.9502	1.0025	0.9
T2	0.9401	0.9302	0.9806	0.9549	0.9
T3	0.9550	0.9693	0.9458	0.9081	0.9

RUN REGRESSION CALCULATIONS
USING ALL LATEX TYPE CURVES

LOW SIZE UNCORRECTED
Regression Output:

Constant	38.6524
Std Err of Y Est	8.6623
R Squared	0.5649
No. of Observations	5.0000
Degrees of Freedom	3.0000
X Coefficient(s)	-5.4063
Std Err of Coef.	2.7393

LOW SIZE CORRECTED
Regression Output:

Constant	28.69
Std Err of Y Est	4.21
R Squared	0.50
No. of Observations	5.00
Degrees of Freedom	3.00
X Coefficient(s)	-2.3294
Std Err of Coef.	1.3325

HIGH SIZE UNCORRECTED
Regression Output:

Constant	40.2778
Std Err of Y Est	2.2305
R Squared	0.9454
No. of Observations	5.0000
Degrees of Freedom	3.0000
X Coefficient(s)	-5.0857
Std Err of Coef.	0.7054

HIGH SIZE CORRECTED
Regression Output:

Constant	24.15
Std Err of Y Est	1.89
R Squared	0.54
No. of Observations	5.00
Degrees of Freedom	3.00
X Coefficient(s)	-1.1405
Std Err of Coef.	0.6002

MYLAR UNCORRECTED
Regression Output:

Constant	48.5167
Std Err of Y Est	4.8113
R Squared	0.7818
No. of Observations	5.0000
Degrees of Freedom	3.0000
X Coefficient(s)	-4.9881
Std Err of Coef.	1.5215

MYLAR CORRECTED
Regression Output:

Constant	37.8
Std Err of Y Est	1.1
R Squared	0.6
No. of Observations	5.0
Degrees of Freedom	3.0
X Coefficient(s)	0.8532
Std Err of Coef.	0.3721

OMNICON 3600 MEASUREMENT REPORT
1:03 P.M. on Fri., Mar. 31, 1989
Calibration : 1x 2.6459E-02 mm²/pp
SAMPLE NAME : Low Size

	Percent Area
Field 1	10.943

Count:	1
Min:	10.943
Max:	10.943
Total:	10.943
Mean:	10.943
StDev:	0.0

End Of Measurement.

OMNICON 3600 MEASUREMENT REPORT
1:00 P.M. on Fri., Mar. 31, 1989
Calibration : 1x 2.6459E-02 mm²/pp
SAMPLE NAME : High Size

	Percent Area
Field 1	15.594

Count:	1
Min:	15.594
Max:	15.594
Total:	15.594
Mean:	15.594
StDev:	0.0

End Of Measurement.

GURLEY POROSITY DATA

HIGH SIZE	LOW SIZE
23.5	31.6
24.5	30.8
22.8	28.7
25.6	30.8
25.2	32.1

K and N BRIGHTNESS REDUCTION DATA

BASE SHEET	ORIGINAL BRIGHTNESS	K and N BRIGHTNESS
LOW SIZE	83.18	33.50
	84.22	33.06
HIGH SIZE	84.45	31.33
	83.39	32.39

COAT WEIGHT DATA

SHEET TYPE	LATEX TYPE VISCOSITY CORRECTED=C UNCORRECTED=U	WEIGHT OF COATING grams/9sqin	COAT WEIGHT lb/R R=3000ft2	AVERAC OF EAC VISCOS TYPE
LOW SIZE	A/C	0.1860	19.6652	
LOW SIZE	B/C	0.1830	19.3480	
LOW SIZE	C/C	0.1710	18.0793	18.96
LOW SIZE	D/C	0.1880	19.8767	
LOW SIZE	E/C	0.1690	17.8678	
LOW SIZE	A/U	0.1500	15.8590	
LOW SIZE	B/U	0.1390	14.6960	
LOW SIZE	C/U	0.1240	13.1101	15.30
LOW SIZE	D/U	0.1530	16.1762	
LOW SIZE	E/U	0.1580	16.7048	
HIGH SIZE	A/C	0.1790	18.9251	
HIGH SIZE	B/C	0.1680	17.7621	
HIGH SIZE	C/C	0.1660	17.5507	17.8
HIGH SIZE	D/C	0.1780	18.8194	
HIGH SIZE	E/C	0.1550	16.3877	
HIGH SIZE	A/U	0.1490	15.7533	
HIGH SIZE	B/U	0.1430	15.1189	
HIGH SIZE	C/U	0.1590	16.8106	16.6
HIGH SIZE	D/U	0.1730	18.2907	
HIGH SIZE	E/U	0.1620	17.1278	
MYLAR	A/C	0.1950	20.6167	
MYLAR	B/C	0.1830	19.3480	
MYLAR	C/C	0.1780	18.8194	19.8
MYLAR	D/C	0.1870	19.7709	
MYLAR	E/C	0.1970	20.8282	
MYLAR	A/U	0.1720	18.1850	
MYLAR	B/U	0.1770	18.7137	
MYLAR	C/U	0.1640	17.3392	17.6
MYLAR	D/U	0.1740	18.3965	
MYLAR	E/U	0.1490	15.7533	

FIGURE 1

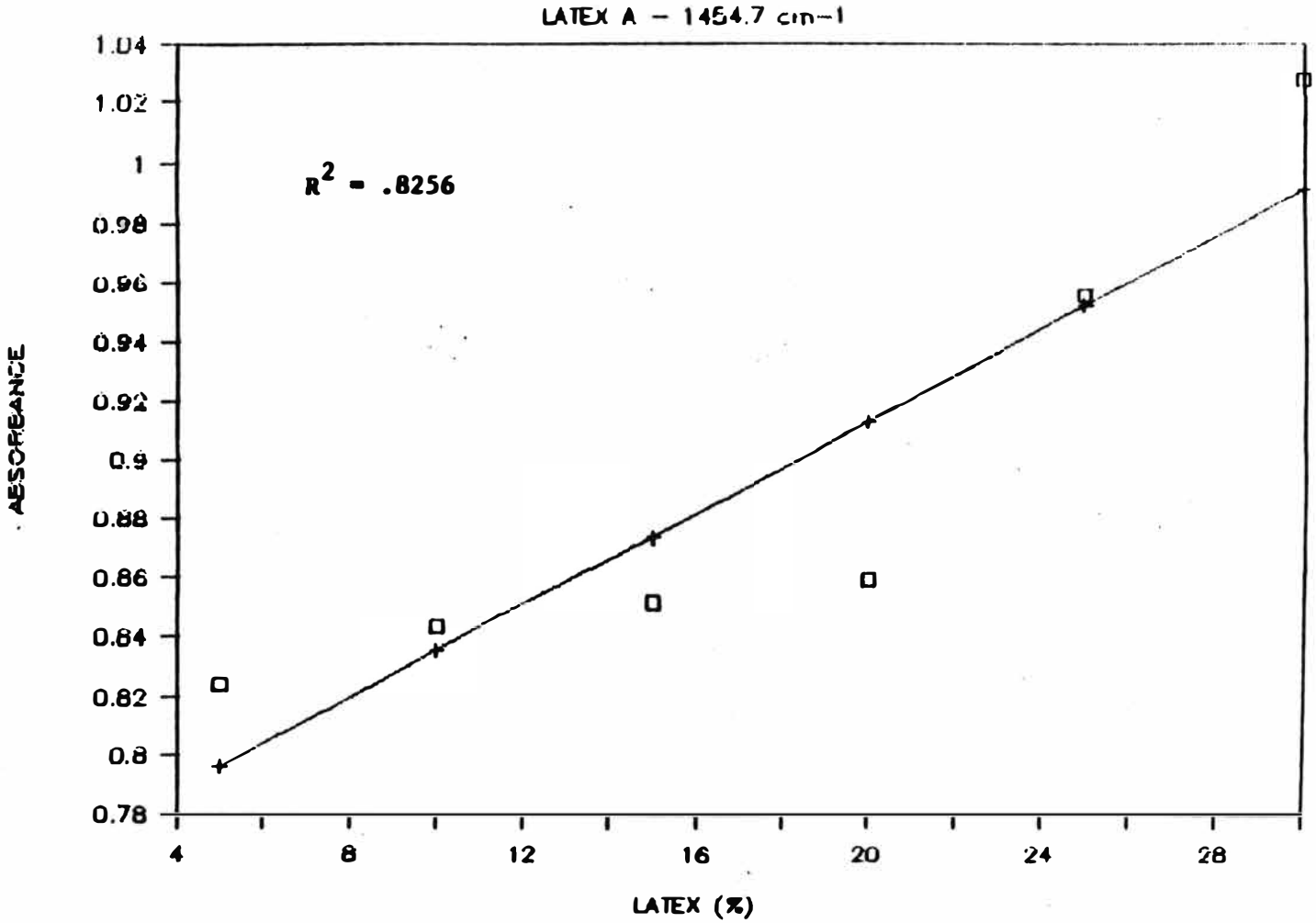
LATEX A - 1454.7 cm-1
R^2 = .8256
ABSORBANCE
1.04
1.02
1
0.98
0.96
0.94
0.92
0.9
0.88
0.86
0.84
0.82
0.8
0.78
4
8
12
16
20
24
28
LATEX (%)

FIGURE 2

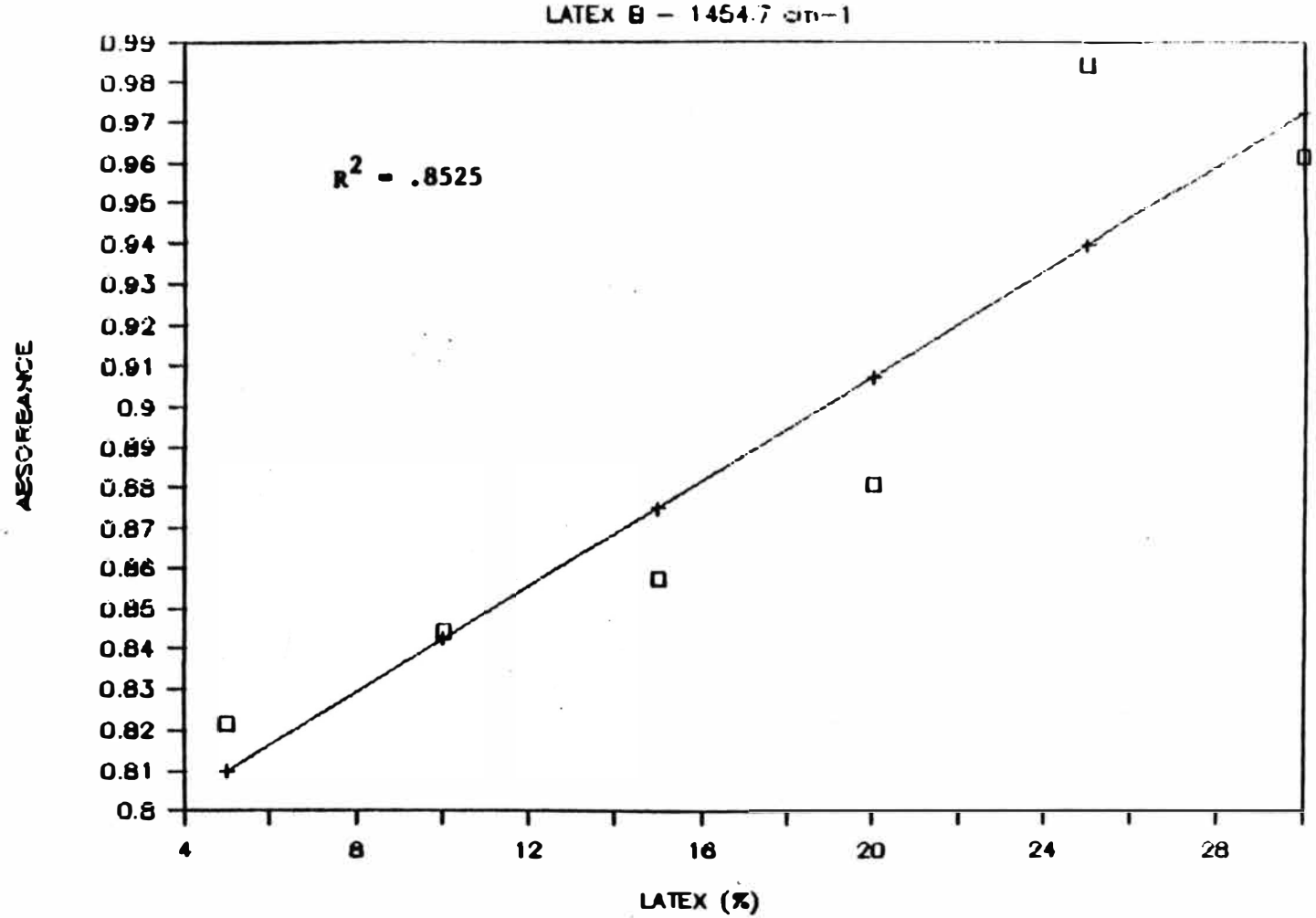
LATEx B – 1454.7 cm-1
R^2 = .8525
ABSORBANCE
0.99
0.98
0.97
0.96
0.95
0.94
0.93
0.92
0.91
0.9
0.89
0.88
0.87
0.86
0.85
0.84
0.83
0.82
0.81
0.8
4
8
12
16
20
24
28
LATEX (%)

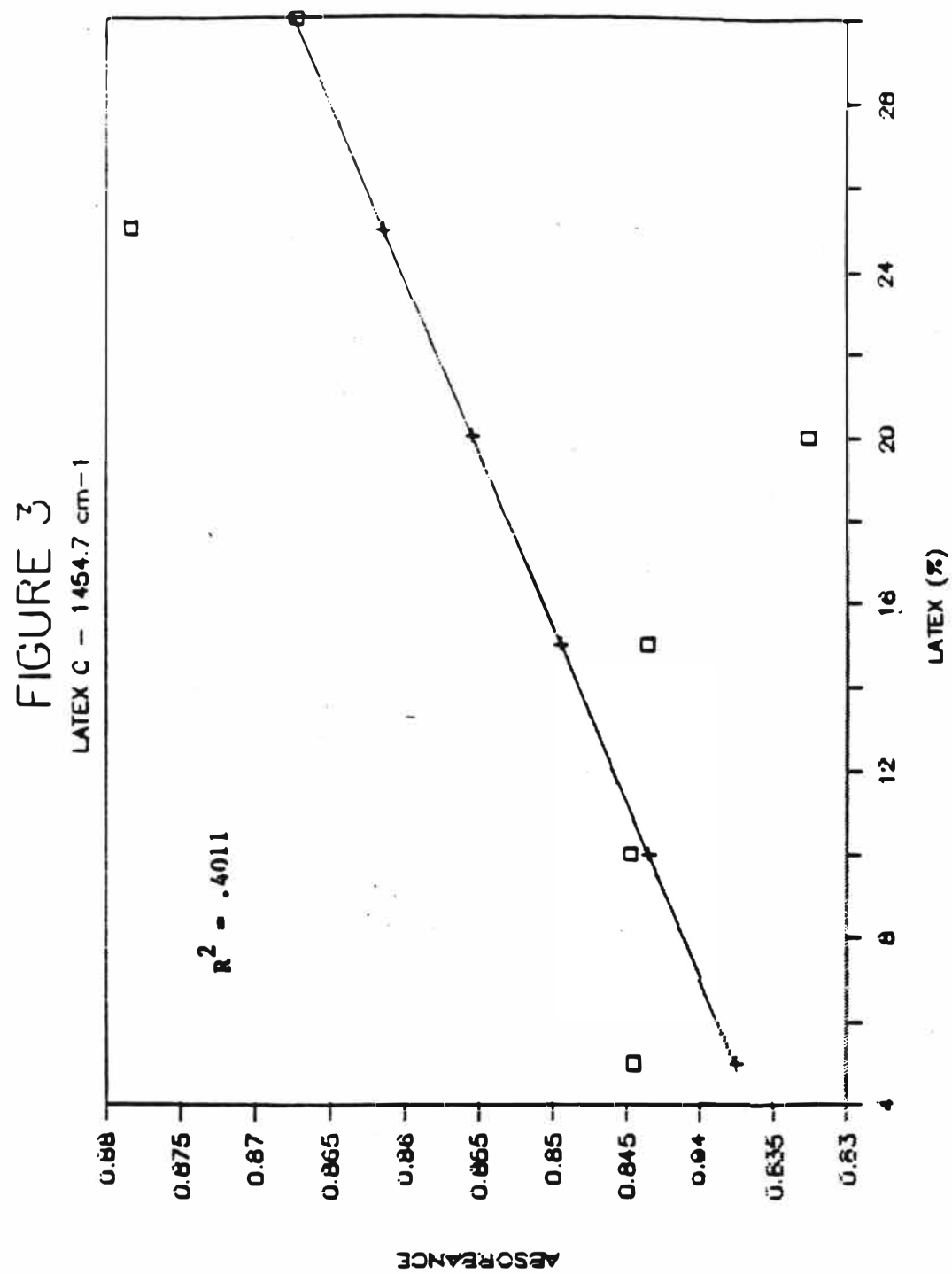
FIGURE 3
LATEX C - 1454.7 cm-1
R^2 = .4011
ABSORBANCE
LATEX (%)
0.88
0.875
0.87
0.865
0.86
0.855
0.85
0.845
0.84
0.835
0.83
4
8
12
16
20
24
28

FIGURE 4

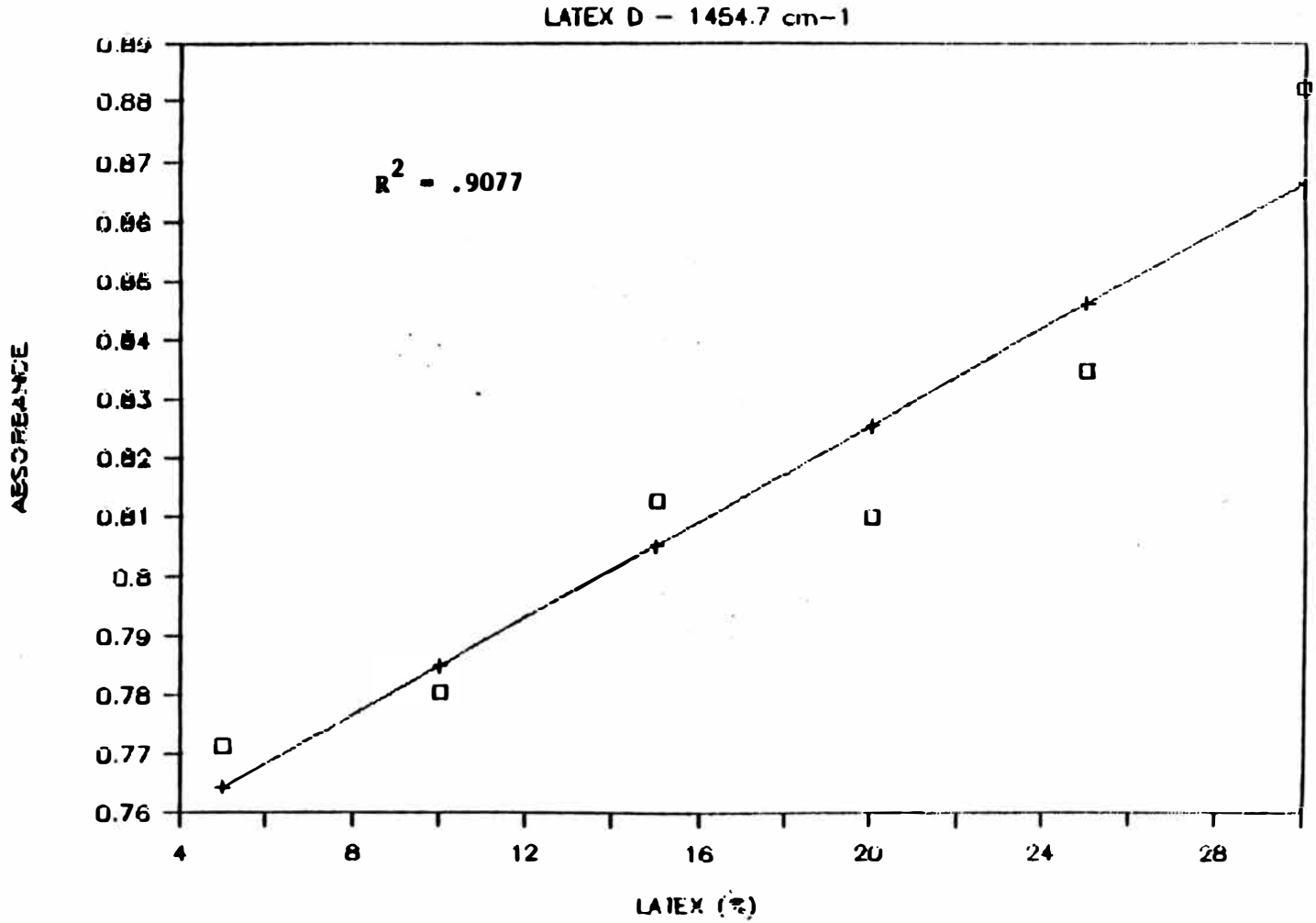
LATEX D - 1454.7 cm-1
R^2 = .9077
ABSORBANCE
0.89
0.88
0.87
0.86
0.85
0.84
0.83
0.82
0.81
0.8
0.79
0.78
0.77
0.76
4
8
12
16
20
24
28
LATEX (%)

FIGURE 5

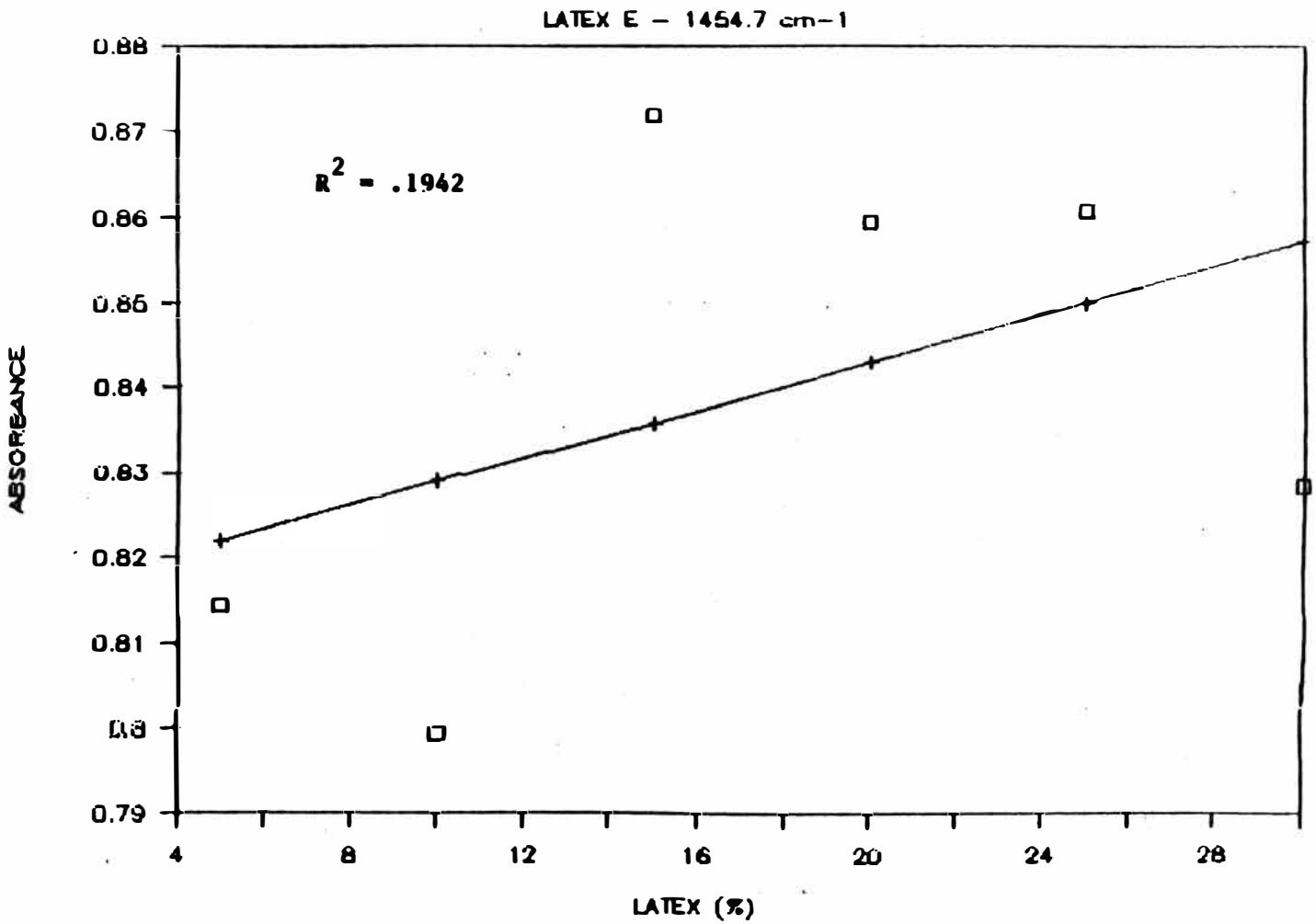
LATEX E – 1454.7 cm-1
R^2 = .1942
ABSORBANCE
0.88
0.87
0.86
0.85
0.84
0.83
0.82
0.81
0.80
0.79
4
8
12
16
20
24
28
LATEX (%)

INSTRUCTIONS

The Model 300 ATR is continuously variable between the angles of 30° and 60°. The optical pathlength remains constant through all angles and is equal to the distance traversed through the sample chamber without the Model 300 inserted in the spectrophotometer. The result is no atmospheric unbalance caused by the Model 300.

Alignment for maximum energy throughput:

a) Set the crystal in the holder as shown in figure. Set the holder (without sample) on the top plate pins in the position shown in figure. The center line of the crystal face should be at the center of the pivot pin.

b) Lock the "Set Angle" at the angle on the face of the prism (usually 45°).

c) Using a white card in front of M2, use the mirror adjusting tool to rotate M1 until the energy beam appears to be at the center of mirror M2.

d) Using the mirror adjusting tool, carefully rotate M2 until transmission throughput is maximum.

e) Using a screwdriver, carefully adjust the "tilt" in mirror M1. This is done by rotating the tilt adjustment screw very slowly clockwise or counter clockwise to see if tilt adjustment is necessary. Adjust tilt as required.

f) Likewise adjust the tilt of M2.

g) At this point transmission throughput should be a maximum. A "background scan" can now be run and the holder can be removed and sample inserted.

MODEL 300 ATR(MIR)

Optical layout at the 45° position

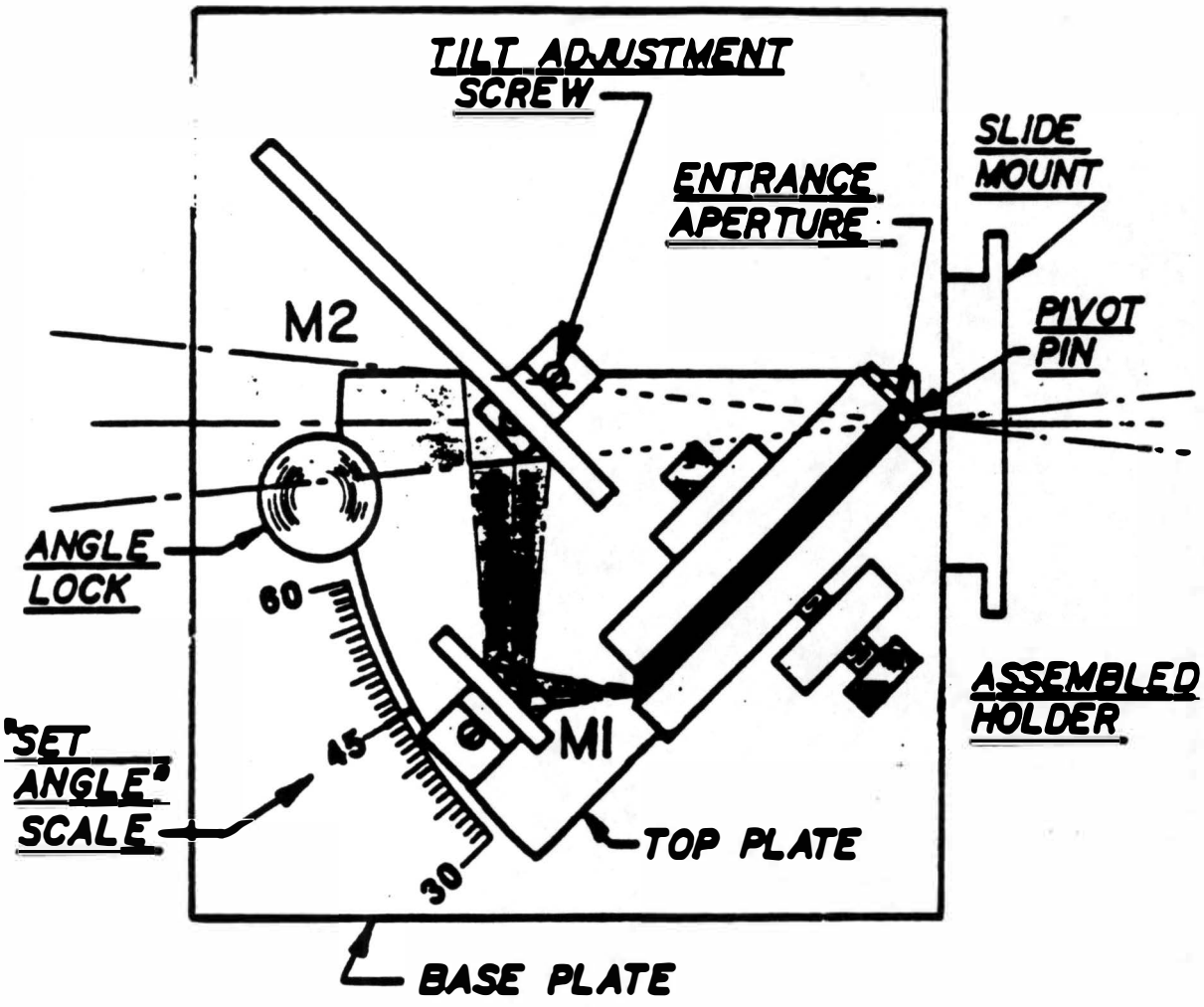

APPENDIX 10-1

CALIBRATION CURVE
5% LATEX DATA

One-Way Analysis of Variance

Data: DATA

Level codes: LATEX

Labels:

Range test: Conf. Int. Confidence level: 95

Analysis of variance

Source of variation	Sum of Squares	d.f.	Mean square	F-ratio	Sig. l
Between groups	.0058974	4	.0014744	3.260	.05
Within groups	.0045229	10	.0004523		
Total (corrected)	.0104203	14			

0 missing value(s) have been excluded.

Table of means for DATA by LATEX

Level	Count	Average	Stnd. Error (internal)	Stnd. Error (pooled s)	95 Percent Confide intervals for me	
A	3	1.0593000	.0238563	.0122786	1.0319343	1.086
B	3	1.0847667	.0028990	.0122786	1.0574010	1.112
C	3	1.0893000	.0100530	.0122786	1.0619343	1.116
D	3	1.1211333	.0063669	.0122786	1.0937677	1.148
E	3	1.0821333	.0058896	.0122786	1.0547677	1.109
Total	15	1.0873267	.0054911	.0054911	1.0750884	1.099

APPENDIX 10-2

CALIBRATION CURVE
10% LATEX DATA

One-Way Analysis of Variance

Data: DATA

Level codes: LATEX

Labels:

Range test: Conf. Int. Confidence level: 95

Analysis of variance

Source of variation	Sum of Squares	d.f.	Mean square	F-ratio	Sig. l
Between groups	.0084305	4	.0021076	7.271	.0(
Within groups	.0028987	10	.0002899		
Total (corrected)	.0113292	14			

0 missing value(s) have been excluded.

Table of means for DATA by LATEX

Level	Count	Average	Stnd. Error (internal)	Stnd. Error (pooled s)	95 Percent Confid intervals for m	
A	3	1.0596000	.0065615	.0098297	1.0376922	1.08
B	3	1.1099000	.0180773	.0098297	1.0879922	1.13
C	3	1.0902333	.0098294	.0098297	1.0683255	1.11
D	3	1.1215333	.0030996	.0098297	1.0996255	1.14
E	3	1.0677333	.0026548	.0098297	1.0458255	1.08
Total	15	1.0898000	.0043960	.0043960	1.0800025	1.09

APPENDIX 10-3

CALIBRATION CURVE
15% LATEX DATA

One-Way Analysis of Variance

Data: DATA

Level codes: LATEX

Labels:

Range test: Conf. Int. Confidence level: 95

Analysis of variance

Source of variation	Sum of Squares	d.f.	Mean square	F-ratio	Sig. l
Between groups	.0092123	4	.0023031	2.169	.1
Within groups	.0106170	10	.0010617		
Total (corrected)	.0198293	14			

0 missing value(s) have been excluded.

Table of means for DATA by LATEX

Level	Count	Average	Stnd. Error (internal)	Stnd. Error (pooled s)	95 Percent Confid intervals for m	
A	3	1.0800000	.0083339	.0188122	1.0380726	1.12
B	3	1.1182667	.0116575	.0188122	1.0763393	1.16
C	3	1.0959000	.0043267	.0188122	1.0539726	1.13
D	3	1.1434667	.0301712	.0188122	1.1015393	1.18
E	3	1.1407333	.0252016	.0188122	1.0988060	1.18
Total	15	1.1156733	.0084131	.0084131	1.0969228	1.13

CALIBRATION CURVE
20% LATEX DATA

One-Way Analysis of Variance

Data: DATA

Level codes: LATEX

Labels:

Range test: Conf. Int. Confidence level: 95

Analysis of variance

Source of variation	Sum of Squares	d.f.	Mean square	F-ratio	Sig. l
Between groups	.0206125	4	.0051531	5.407	.01
Within groups	.0095302	10	.0009530		
Total (corrected)	.0301427	14			

0 missing value(s) have been excluded.

Table of means for DATA by LATEX

Level	Count	Average	Stnd. Error (internal)	Stnd. Error (pooled s)	95 Percent Confide intervals for me	
A	3	1.0785667	.0190054	.0178234	1.0388431	1.118
B	3	1.1387333	.0082281	.0178234	1.0990098	1.178
C	3	1.0645000	.0148291	.0178234	1.0247764	1.104
D	3	1.1597333	.0016455	.0178234	1.1200098	1.199
E	3	1.1357333	.0306080	.0178234	1.0960098	1.175
Total	15	1.1154533	.0079709	.0079709	1.0976884	1.133

APPENDIX 10-5

CALIBRATION CURVE
25% LATEX DATA

One-Way Analysis of Variance

Data: DATA

Level codes: LATEX

Labels:

Range test: Conf. Int. Confidence level: 95

Analysis of variance

Source of variation	Sum of Squares	d.f.	Mean square	F-ratio	Sig.
Between groups	.0144815	4	.0036204	3.285	.03
Within groups	.0110194	10	.0011019		
Total (corrected)	.0255009	14			

0 missing value(s) have been excluded.

Table of means for DATA by LATEX

Level	Count	Average	Stnd. Error (internal)	Stnd. Error (pooled s)	95 Percent Confid intervals for m	
A	3	1.1723667	.0065839	.0191655	1.1296520	1.21
B	3	1.2073667	.0240822	.0191655	1.1646520	1.25
C	3	1.1248000	.0177697	.0191655	1.0820853	1.16
D	3	1.1853333	.0113936	.0191655	1.1426186	1.22
E	3	1.1342000	.0277073	.0191655	1.0914853	1.17
Total	15	1.1648133	.0085711	.0085711	1.1457107	1.18

APPENDIX 10-6

CALIBRATION CURVE
30% LATEX DATA

One-Way Analysis of Variance

Data: DATA

Level codes: LATEX

Labels:

Range test: Conf. Int. Confidence level: 95

Analysis of variance

Source of variation	Sum of Squares	d.f.	Mean square	F-ratio	Sig. l
Between groups	.0586744	4	.0146686	11.584	.00
Within groups	.0126630	10	.0012663		
Total (corrected)	.0713375	14			

0 missing value(s) have been excluded.

Table of means for DATA by LATEX

Level	Count	Average	Stnd. Error (internal)	Stnd. Error (pooled s)	95 Percent Confid intervals for me	
A	3	1.2515333	.0088706	.0205451	1.2057438	1.29
B	3	1.2408333	.0255804	.0205451	1.1950438	1.28
C	3	1.1085333	.0195604	.0205451	1.0627438	1.15
D	3	1.1829333	.0086457	.0205451	1.1371438	1.22
E	3	1.1048333	.0303333	.0205451	1.0590438	1.15
Total	15	1.1777333	.0091880	.0091880	1.1572556	1.19

APPENDIX 11-1

MYLAR BASE

STATISTICAL ANALYSIS

Table of means for PETE1.DATA

Level	Count	Average	Stnd. Error (internal)	Stnd. Error (pooled s)	95 Percent Confide for mean	
PETE1.LATEX						
A	6	.9509333	.0046891	.0091173	.9319103	.969
B	6	.9484333	.0081345	.0091173	.9294103	.967
C	6	.9540333	.0067469	.0091173	.9350103	.973
D	6	.9336667	.0160556	.0091173	.9146436	.952
E	6	.9149000	.0228189	.0091173	.8958770	.933
PETE1.VISCOSITY						
C	15	.9548667	.0057174	.0057663	.9428355	.966
U	15	.9259200	.0098941	.0057663	.9138888	.937
PETE1.LATEX by PETE1.VISCOSITY						
A C	3	.9508333	.0054112	.0128938	.9239307	.977
A U	3	.9510333	.0089804	.0128938	.9241307	.977
B C	3	.9455333	.0120491	.0128938	.9186307	.972
B U	3	.9513333	.0133138	.0128938	.9244307	.978
Total	30	.9403933	.0040774	.0040774	.9318860	.948

Analysis of Variance for PETE1.DATA

Source of variation	Sum of Squares	d.f.	Mean square	F-ratio	Sig.
MAIN EFFECTS	.0126260	5	.0025252	5.063	.0
PETE1.LATEX	.0063416	4	.0015854	3.179	.0
PETE1.VISCOSITY	.0062843	1	.0062843	12.600	.0
2-FACTOR INTERACTIONS	.0111055	4	.0027764	5.567	.0
PETE1.LATEPETE1.VISC	.0111055	4	.0027764	5.567	.0
RESIDUAL	.0099751	20	4.98754E-004		
TOTAL (CORR.)	.0337065	29			

0 missing values have been excluded.

APPENDIX 11-2

HIGH SIZE BASE

STATISTICAL ANALYSIS

Table of means for PETE2.DATA

Level	Count	Average	Stnd. Error (internal)	Stnd. Error (pooled s)	95 Percent Confide for mean	
PETE2.LATEX						
A	6	.9105167	.0161954	.0070892	.8957234	.925
B	6	.8935833	.0070001	.0070892	.8787920	.908
C	6	.8728833	.0066673	.0070892	.8580920	.887
D	6	.8729333	.0050460	.0070892	.8581420	.887
E	6	.8554667	.0079434	.0070892	.8406754	.870
PETE2.VISCOSITY						
C	15	.8720667	.0033347	.0044836	.8627119	.881
U	15	.8900867	.0096197	.0044836	.8807318	.899
PETE2.LATEX by PETE2.VISCOSITY						
A C	3	.8848333	.0071669	.0100256	.8639153	.905
A U	3	.9362000	.0245044	.0100256	.9152820	.957
B C	3	.8807000	.0023431	.0100256	.8597820	.901
B U	3	.9064667	.0085752	.0100256	.8855486	.927
Total	30	.8810767	.0031704	.0031704	.8744618	.887

Analysis of Variance for PETE2.DATA

Source of variation	Sum of Squares	d.f.	Mean square	F-ratio	Sig. l
MAIN EFFECTS	.0133101	5	.0026620	8.828	.00
PETE2.LATEX	.0108747	4	.0027187	9.016	.00
PETE2.VISCOSITY	.0024354	1	.0024354	8.077	.0J
2-FACTOR INTERACTIONS	.0048630	4	.0012158	4.032	.0
PETE2.LATEPETE2.VISC	.0048630	4	.0012158	4.032	.0
RESIDUAL	.0060307	20	3.01536E-004		
TOTAL (CORR.)	.0242038	29			

0 missing values have been excluded.

APPENDIX 11-3

LOW SIZE BASE

STATISTICAL ANALYSIS

Table of means for PETE3.DATA

Level	Count	Average	Stnd. Error (internal)	Stnd. Error (pooled s)	95 Percent Confider for mean	
PETE3.LATEX						
A	6	.9177500	.0287540	.0140372	.8834618	.947(
B	6	.8779667	.0171803	.0140372	.8436783	.907.
C	6	.8833500	.0094572	.0140372	.8542518	.912(
D	6	.8674167	.0076968	.0140372	.8381285	.896'
E	6	.8418000	.0039559	.0140372	.8125118	.871(
PETE3.VISCOSITY						
C	15	.8761733	.0058574	.0088779	.8576499	.894(
C	15	.8792200	.0153547	.0088779	.8606965	.897
PETE3.LATEX by PETE3.VISCOSITY						
A C	3	.8764333	.0050900	.0198516	.8350136	.917
A C	3	.9590667	.0489999	.0198516	.9176469	1.000
B C	3	.9056000	.0108099	.0198516	.8641803	.947
B C	3	.8503333	.0244000	.0198516	.8089136	.891
Total	30	.8776967	.0062776	.0062776	.8645986	.890

Analysis of Variance for PETE3.DATA

Source of variation	Sum of Squares	d.f.	Mean square	F-ratio	Sig. l
MAIN EFFECTS	.0182667	5	.0036533	3.090	.03
PETE3.LATEX	.0181971	4	.0045493	3.848	.01
PETE3.VISCOSITY	.0000696	1	.0000696	.059	.81
2-FACTOR INTERACTIONS	.0148737	4	.0037184	3.145	.03
PETE3.LATEPETE3.VISC	.0148737	4	.0037184	3.145	.03
RESIDUAL	.0236452	20	.0011823		
TOTAL (CORR.)	.0567856	29			

0 missing values have been excluded.

APPENDIX 12

KEEGAN COATER SETUP

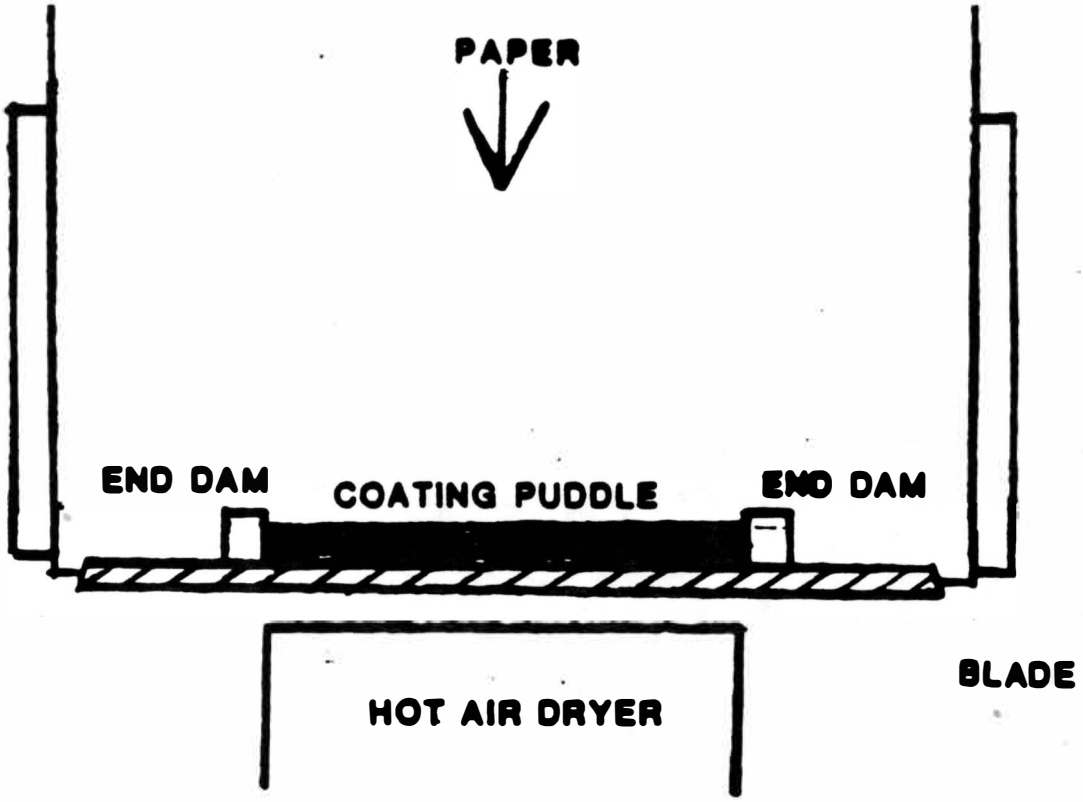

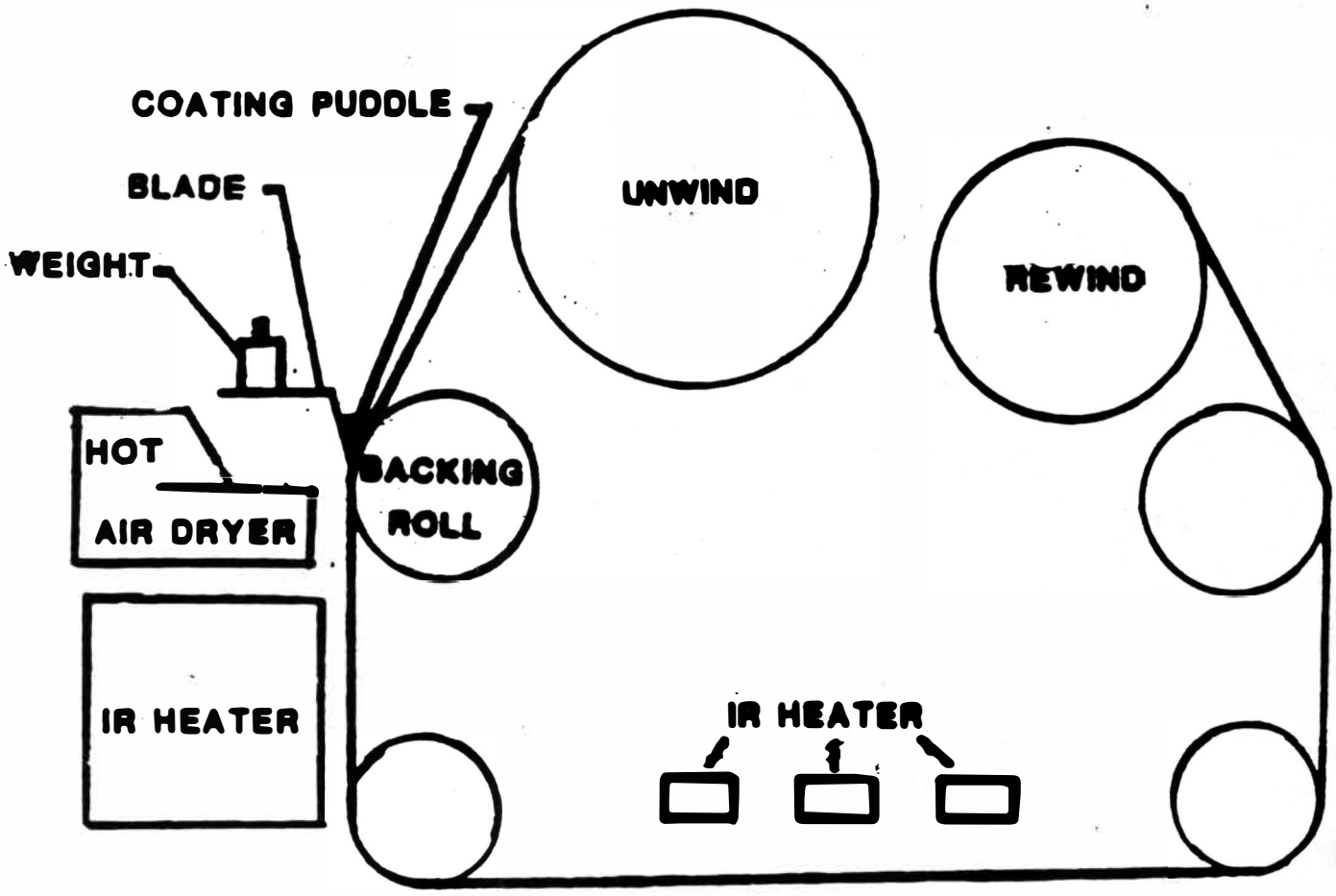

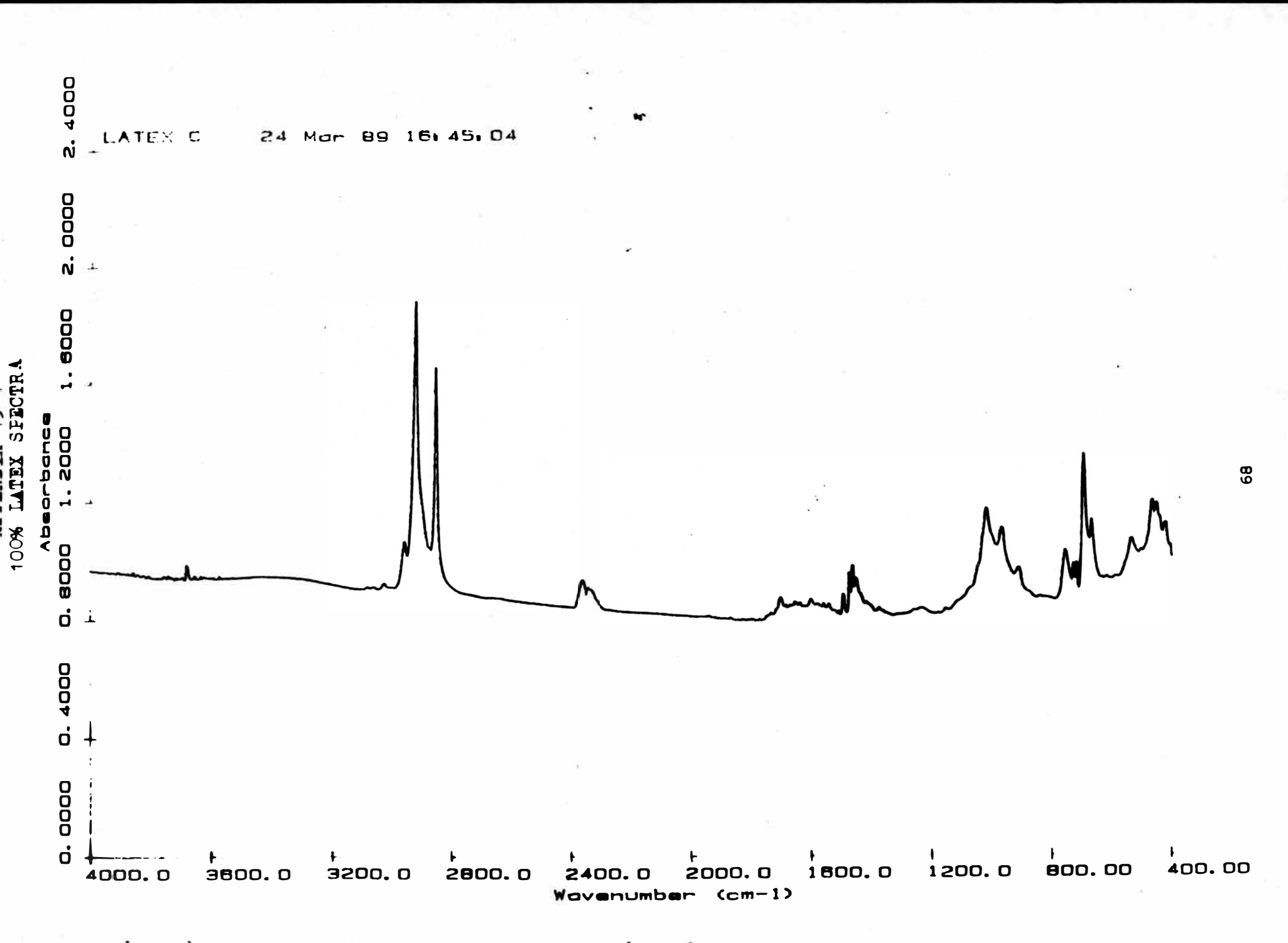

100% LATEX SPECTRA

APPENDIX T5-2
UNCORRECTED TRIAL RUN SPECTRA

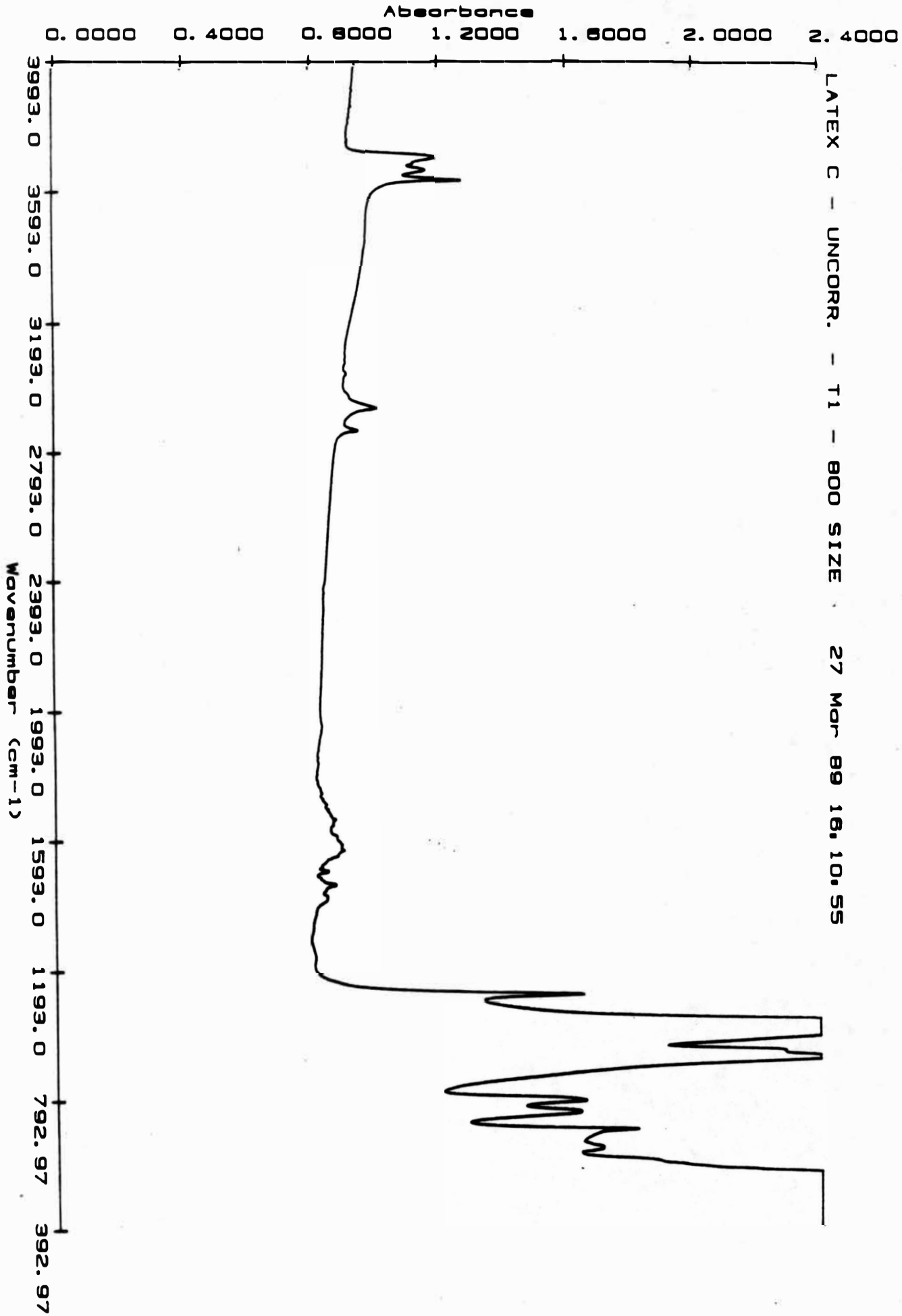

APPENDIX 1(B)

CORRECTED TRIAL RUN SPECTRA

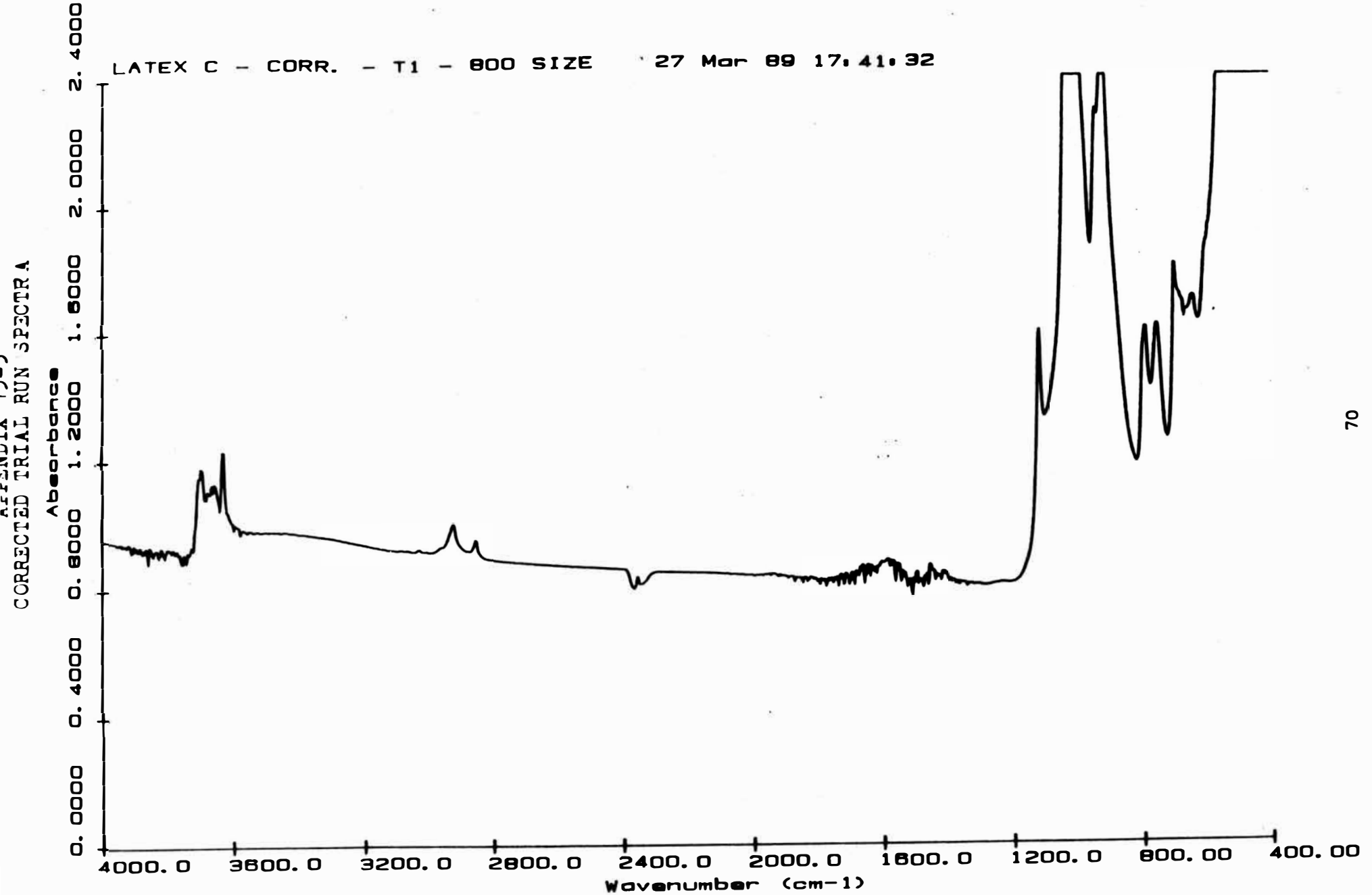

The author

owes the results of this work

to the understanding and love given by his

beautiful wife Lisa

and fine sons

Philip

and

Thomas

PJR

This work is dedicated to

Norbert Jerome and Dolores Rose Rudy

Whose patience has led to a good thing

PJR